WL-TR-96-3098

ENERGY ABSORBING MATERIALS FOR PROTECTIVE STRUCTURES

DAVID L. READ
LARRY C. MUSZYNSKI

APPLIED RESEARCH ASSOCIATES, INC.
Post Office Box 40128
Tyndall AFB FL 32403-1142

AUGUST 1994

FINAL REPORT FOR OCTOBER 1992--JANUARY 1994

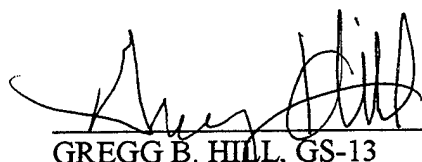## Approved for public release; distribution unlimited

19960708 007

DTIC QUALITY INSPECTED 1

NOTICE

WHEN GOVERNMENT DRAWINGS, SPECIFICATIONS, OR OTHER DATA ARE USED FOR ANY PURPOSE OTHER THAN IN CONNECTION WITH A DEFINITELY GOVERNMENT-RELATED PROCUREMENT, THE UNITED STATES GOVERNMENT INCURS NO RESPONSIBILITY OR ANY OBLIGATION WHATSOEVER. THE FACT THAT THE GOVERNMENT MAY HAVE FORMULATED OR IN ANY WAY SUPPLIED THE SAID DRAWINGS, SPECIFICATIONS, OR OTHER DATA, IS NOT TO BE REGARDED BY IMPLICATION, OR OTHERWISE IN ANY MANNER CONSTRUED, AS LICENSING THE HOLDER, OR ANY OTHER PERSON OR CORPORATION, OR AS CONVEYING ANY RIGHTS OR PERMISSION TO MANUFACTURE, USE, OR SELL ANY PATENTED INVENTION THAT MAY IN ANY WAY BE RELATED THERETO.

THIS REPORT IS RELEASABLE TO THE NATIONAL TECHNICAL INFORMATION SERVICE (NTIS). AT NTIS, IT WILL BE AVAILABLE TO THE GENERAL PUBLIC, INCLUDING FOREIGN NATIONS.

THIS TECHNICAL REPORT HAS BEEN REVIEWED AND IS APPROVED FOR PUBLICATION.

GREGG B. HILL, GS-13
Project Officer

WILLIAM S. STRICKLAND, GS-14
Chief, Pavements and Facilities Section

EDGAR F. ALEXANDER, GS-15
Chief, Air Base Technology Branch

REPORT DOCUMENTATION PAGE

Public reporting burden for this collection of information is estimated to average 1 hour per response, including the time for reviewing instructions, searching existing data sources, gathering and maintaining the data needed, and completing and reviewing the collection of information. Send comments regarding this burden estimate or any other aspect of this collection of information, including suggestions for reducing this burden, to Washington Headquarters Services, Directorate for Information Operations and Reports, 1215 Jefferson Davis Highway, Suite 1204, Arlington, VA 22202-4302, and to the Office of Management and Budget, Paperwork Reduction Project (0704-0188), Washington, DC 20503.

1. AGENCY USE ONLY (Leave blank)	2. REPORT DATE AUGUST 1994	3. REPORT TYPE AND DATES COVERED 10/92 - 01/94

4. TITLE AND SUBTITLE

ENERGY ABSORBING MATERIALS FOR PROTECTIVE STRUCTURES

6. AUTHOR(S)

READ, D.L., MUSZYNSKI, L.C.

5. FUNDING NUMBERS

F08635-93-C-0020
PE   63723
PR   2104
TA   20
WU   01

7. PERFORMING ORGANIZATION NAME(S) AND ADDRESS(ES)

Applied Research Associates, Inc.
Post Office Box 40128
Tyndall AFB FL 32403-1148

8. PERFORMING ORGANIZATION REPORT NUMBER

9. SPONSORING/MONITORING AGENCY NAME(S) AND ADDRESS(ES)

WL/FIVCO-OL
139 Barnes Drive Suite 2
Tyndall AFB FL 32403-5323
POC: W.S. Strickland, WL/FIVCO-OL
904-283-3709

Flight Dynamics Directorate
Wright Laboratory
Air Force Materiel Command
WPAFB OH 45433-7562

10. SPONSORING/MONITORING AGENCY REPORT NUMBER

WL-TR-96-3098

11. SUPPLEMENTARY NOTES

13. ABSTRACT (Maximum 200 words)

THIS REPORT DOCUMENTS PHASE II OF A THREE-PHASE EFFORT TO DEVELOP FIBER- AND REBAR- REINFORCED CONCRETE BEAM DESIGNS AND ASSOCIATED DESIGN METHODS THAT CAN BE USED IN THE CONSTRUCTION OF HARDENED STRUCTURES TO INCREASE THEIR SURVIVABILITY, WHILE REDUCING THEIR COST AND WEIGHT. IN PARTICULAR, THIS WORK WILL BENEFIT BARE BASE MODULAR, PREFABRICATED, RAPIDLY ERECTABLE HARDENED STRUCTURES WHERE WEIGHT SAVING AND INCREASED MATERIAL TOUGHNESS ARE CRITICAL ISSUES.

14. SUBJECT TERMS

ENERGY ABSORBING G MATERIALS, PROTECTIVE CONSTRUCTION, FIBER REINFORCED CONCRETE

15. NUMBER OF PAGES

60

16. PRICE CODE

17. SECURITY CLASSIFICATION OF REPORT UNCLASSIFIED	18. SECURITY CLASSIFICATION OF THIS PAGE UNCLASSIFIED	19. SECURITY CLASSIFICATION OF ABSTRACT UNCLASSIFIED	20. LIMITATION OF ABSTRACT SAR

TABLE OF CONTENTS

TABLE OF CONTENTS (CONCLUDED)

LIST OF FIGURES

LIST OF TABLES

EXECUTIVE SUMMARY

A. OBJECTIVE

This technical report documents Phase II of a three-phase research and testing effort undertaken by the Airbase Survivability Section (FIVCS), Airbase Systems Branch (FIVC), Vehicle Subsystems Division (FIV), of the Flight Dynamics Directorate of Wright Laboratory to develop fiber- and rebar-reinforced concrete beam designs and associated design methods that can be used in construction of hardened structures to increase their survivability, while reducing their cost and weight. In particular, this work will benefit bare base, modular, prefabricated, rapidly erectable hardened structures where weight saving and increased material toughness, i.e., energy absorption per unit weight, are critical issues. In addition, using precast fiber- and rebar-reinforced concrete structural members will allow fiber content, concrete strength, and quality to be controlled, while minimizing construction time and cost.

The objective of Phase II of this technical effort was to carry out large-scale tests of the most promising beam candidates identified in the previous Phase I small-scale beam testing program conducted by FIVCS in 1991-92. Large-scale beam tests were conducted in Phase II of this effort to ensure no scaling factor significantly influenced the promising structural performance of fiber- and rebar-reinforced beam designs identified during the Phase I testing program. In Phase III of this technical effort, fiber- and rebar-reinforced concrete beam designs will be optimized and associated design procedures developed. The final objective of this effort is to incorporate the resulting beam designs and design methods into the Defense Nuclear Agency's joint services manual, <u>Design and Analysis of Hardened Structures to Conventional Weapon Effects (DAHS CWE Manual)</u>, (Reference 1).

B. BACKGROUND

As shown in operation Desert Storm, hardened structures housing mission-critical assets are susceptible to severe damage or total destruction from "smart" conventional weapons. In addition, significant damage can be done to a hardened structure by a near miss of a standard conventional weapon or a direct hit. Also, during operation Desert Storm, many, if not most, U.S. military mission-critical assets were deployed to bases where hardened structures were in limited supply or not available. Without the protection of hardened structures, mission-critical assets are extremely vulnerable to damage from attack by conventional weapons (bombs, artillery, rockets, small-arms, etc.).

Typically, airbase hardened structures house mission-critical assets, such as command, control, and communications (C^3) centers, personnel, aircraft, munitions, critical equipment and supplies, etc. The current vulnerability of hardened structures at forward operating bases (FOBs), and the possible lack of them at bare bases when force projection is required jeopardizes the ability of either type of airbase to fulfill its mission after an attack. To address the problem of ensuring that an airbase fulfills its wartime mission, the U. S. Air Force developed the Airbase Operability (ABO) concept. ABO consists of five phases: (1) defense, (2) survival, (3) recovery, (4) aircraft sortie generation, and (5) sortie support.

As part of the survival phase of ABO, the U.S. Air Force is constantly searching for ways to improve the performance, i.e., survivability, of hardened structures, while at the same time, if possible, reducing their construction cost and weight. In addition, to address the possible lack of hardened structures at bare bases, the U.S. Air Force is developing prefabricated, modular, rapidly erectable hardened structures. As part of these research efforts, a small-scale beam testing program was conducted by FIVCS in 1991-92 to determine whether using fiber-reinforcement in combination with standard rebar-reinforcement in lightweight concrete beams could minimize, or possibly eliminate the need for shear and compression reinforcement in the beams, while at the same time enhancing the performance of the beams as defined by material toughness. Results from this small-scale beam testing program were very promising. Consequently, FIVCS undertook a large-scale beam testing program, to first verify the results of the best beam designs from the small-scale testing program, and secondly to optimize the best beam designs and develop associated design procedures.

C.   SCOPE

During Phase II testing, five beam types were assessed, with 3 beams of each type tested on a load-frame to generate load-deflection curves. In addition, for each beam type, two subsets of beams were tested. Two beams of each type were instrumented with vibrating wire rebar strain gages cast in the beams during fabrication. The remaining beam of each type used standard rebar. The load-deflection curves generated for each beam type were used to assess each type's ductility and overall material toughness. Based on ductility and overall material toughness, the best beam types were selected for Phase III testing, along with new promising beam designs as they arise.

D.   RESULTS

1.   Beam Testing and Best Beam Types

Beam testing emphasized lightweight, high strength concrete. The overall goal of beam testing was to determine whether lightweight, high-strength concrete beams with fiber

reinforcement in combination with standard rebar reinforcement could provide superior performance to a baseline beam. The baseline beam was a standard weight beam designed according to current hardened construction criteria, i.e., symmetrically reinforced with stirrup shear reinforcement. In addition, testing was structured to determine whether, by using fiber reinforcement, standard rebar compression and shear (stirrup) reinforcement could be eliminated without degrading beam performance. Tested beam types were compared based on load-deflection curves generated under static flexural third-point loading. Using these curves, ductility index, energy ratio, and energy absorption per unit weight were computed for each beam type. These values allowed comparisons to be made between beam types with respect to material ductility and energy absorption characteristics. Results from this beam testing showed that two of the five beam types provided the best overall performance. The best beam types are:

- Beam Type SR8: lightweight, high-strength concrete with tension rebar reinforcement, in combination with straight, short (5/8-inch) steel fiber reinforcement.

- Beam Type M2: lightweight, high-strength concrete with tension rebar reinforcement, in combination with anchorloc steel fibers and mat fiber matrix in the bottom of the beam.

2. Compression and Shear Reinforcement Replacement

Static test results indicate that use of fiber reinforcement will eliminate the need for compression and shear reinforcement in lightweight concrete beams, without degrading their performance. However, dynamic testing should be accomplished to verify this conclusion. Replacing compression and shear reinforcement provides two primary benefits to hardened structure construction. The first is a weight saving in concrete structural members. The second is a cost saving, which is always an issue with hardened structures.

3. Spalling

The final benefit of using fiber-reinforced concrete in hardened structures is minimization of spalling. Using fiber reinforcement significantly reduces the chance of spalling when concrete is subjected to impact or blast effects, (Reference 2). Spalling of the inside walls of a hardened structure from blast and/or impact poses a significant hazard to personnel and equipment within the structure. Minimizing spalling is another critical consideration in the design of hardened structures.

E. CONCLUSIONS

Using fiber reinforcement in combination with standard reinforcement in hardened structures would provide a significant performance enhancement over the conventionally

reinforced concrete structural members currently used in hardened construction. The major benefits are threefold. First, the ductility and energy absorption characteristics, i.e., material toughness, of the highest-rated lightweight, fiber- and rebar-reinforced concrete beam types are clearly superior to the standard weight, symmetrically-reinforced baseline beam type that represents current U.S. Air Force hardened structure design practice. Second, using fibers will eliminate the need for compression and shear reinforcement in lightweight concrete beams, without degrading their performance, while providing a weight saving of approximately 15-percent. Also, eliminating compression and shear reinforcement would further reduce the cost and weight of the concrete beams. Third, including fibers would minimize, or possibly eliminate, spalling of the interior walls of a hardened structure from blast loading or projectile impact.

F.   RECOMMENDATIONS

Based on test results, using fiber reinforcement in combination with standard rebar reinforcement should be a design option for future U.S. Air Force hardened structures. This recommendation holds true especially for modular, prefabricated, rapidly erectable hardened shelters. Once the final phase of this research effort is completed by the end of 1994, all the necessary tools and information, such as design methods and mix designs, will be available for using fiber reinforcement in hardened structures. Finally, scaled hardened structures should be constructed using the most promising fiber- and rebar-reinforced structural member designs identified by this technical effort. The scaled structures should be instrumented with accelerometers, pressure gauges, etc. A baseline, scaled, instrumented structure should also be constructed using current hardened construction design practices. The structures should then be subjected to blast loadings and dynamic impacts from conventional weapons, such as bombs and rockets. Based on instrumentation data, visual inspection, and deflection measurements, the relative performance of the scaled structures can be determined. Successful completion of this testing effort should provide indisputable proof that fiber- and rebar-reinforced concrete structural members are superior to the standard rebar-only reinforced structural members currently used in U.S. Air Force hardened structures.

SECTION 1

INTRODUCTION

1.1 OBJECTIVE

This technical report documents Phase II of a three-phase research and testing effort undertaken by the Airbase Survivability Section (FIVCS), Airbase Systems Branch (FIVC), Vehicle Subsystems Division (FIV), of the Flight Dynamics Directorate of Wright Laboratory to develop fiber- and rebar-reinforced concrete beam designs and associated design methods that can be used in constructing hardened structures to increase their survivability, while reducing their cost and weight. In particular, this work will benefit bare base, modular, prefabricated, rapidly erectable hardened structures where weight saving and increased material toughness, i.e. energy absorption per unit weight, are critical issues. In addition, using precast fiber- and rebar-reinforced concrete structural members will allow fiber content, concrete strength, and quality to be controlled, while minimizing construction time and cost. Because precast construction is envisioned for modular, fiber-reinforced hardened structures, such issues as field constructability and field quality control management were not considered critical when developing beam designs/methods during this research effort. However, using fibers in conjunction with standard reinforcement does not preclude cast-in-place hardened structures.

The objective of Phase II of this technical effort was to carry out large-scale tests of the most promising beam candidates identified in the previous Phase I small-scale beam testing program conducted by FIVCS in CY 1991-92. Results from this Phase I testing program are documented in Reference 3. Large-scale beam tests were conducted in Phase II of this effort to ensure no scaling factor significantly influenced the promising structural performance of fiber- and rebar-reinforced beam designs identified during the Phase I testing program. In Phase III of this technical effort, fiber- and rebar-reinforced beam designs will be optimized and associated design procedures developed. The final objective of this effort is to incorporate the resulting beam designs and design methods into the Defense Nuclear Agency's joint services manual, Design and Analysis of Hardened Structures to Conventional Weapon Effects (DAHS CWE Manual), (Reference 1).

1

1.2 BACKGROUND

As shown in operation Desert Storm, hardened structures housing mission-critical assets are susceptible to severe damage or total destruction from "smart" conventional weapons. In addition, significant damage can be done to a hardened structure by a near miss of a standard conventional weapon or a direct hit, i.e. the golden BB. Also, during operation Desert Storm, many, if not most, U.S. military mission-critical assets were deployed to bases where hardened structures were in limited supply or not available. Without the protection of hardened structures, mission-critical assets are extremely vulnerable to damage from attack by conventional weapons (bombs, artillery, rockets, small-arms, etc.).

Typically, airbase hardened structures house mission-critical assets, such as command, control, and communications (C^3) centers, personnel, aircraft, munitions, critical equipment and supplies, etc. The current vulnerability of hardened structures at forward operating bases (FOBs), and the possible lack of them at bare bases when force projection is required jeopardizes the ability of either type of airbase to fulfill its mission after an attack. To address the problem of ensuring that an airbase fulfills its wartime mission, the U. S. Air Force developed the Airbase Operability (ABO) concept. ABO consists of five phases: (1) defense, (2) survival, (3) recovery, (4) aircraft sortie generation, and (5) sortie support.

As part of the survival phase of ABO, the U.S. Air Force is constantly searching for ways to improve the performance, i.e. survivability, of hardened structures, while at the same time, if possible, reducing their construction cost and weight. In addition, to address the possible lack of hardened structures at bare bases, the U.S. Air Force is developing prefabricated, modular, rapidly erectable hardened structures. As part of these research efforts, a small-scale beam testing program was conducted by FIVCS in CY 1991-92 to determine whether using fiber reinforcement in combination with standard rebar reinforcement in lightweight concrete beams could minimize, or possibly eliminate the need for shear and compression reinforcement in the beams, while at the same time enhancing the performance of the beams as defined by material toughness. Results from this small-scale beam testing program were very promising. Consequently, FIVCS undertook a large-scale beam testing program, first to verify the results of the best beam designs from the small-scale beam testing program, and second to optimize the best beam designs and develop associated design procedures.

1.3 SCOPE

During Phase II testing, five beam types were assessed, with 3 beams of each type tested on a load-frame to generate load-deflection curves. In addition, for each beam type, two subsets of

beams were tested. Two beams of each type were instrumented with vibrating wire rebar strain gages cast in the beams during fabrication. The remaining beam of each type used standard rebar. The load-deflection curves generated for each beam type were used to assess each type's ductility and overall material toughness. Based on ductility and overall material toughness, the best beam types were selected for Phase III testing, along with new promising beam designs as they arise.

1.4 REPORT ORGANIZATION

In Section II of this report, a brief description of the load-frame constructed for this research effort is given, along with general beam testing procedures. In addition, descriptions of the individual beam types are provided. In Section III, test results from the beams instrumented with vibrating wire rebar strain gages are given for each beam type. In Section IV, test results from the beams using standard rebar are given for each beam type. In Section V, conclusions dealing with the feasibility and benefits of using lightweight, fiber- and rebar-reinforced concrete structural members in hardened structures are given. Additionally, recommendations on fielding lightweight, fiber-reinforced concrete mixes and design methods are presented.

SECTION 2

LOAD-FRAME AND BEAM TYPE DESCRIPTIONS

2.1 LOAD-FRAME

2.1.1 General Design

The load-frame, which is shown in Figures 1 and 2, was fabricated from a 20-foot long W24 x 162 "I" beam. The load-frame was designed for a 100,000-pound capacity. Two 50,000-pound capacity Enerpac™ hydraulic rams, attached to the underside of the top "I" beam section, were used to load the concrete beams. At the base of each hydraulic ram was a load cell to measure the loads applied to the concrete beams. A 4-inch wide steel channel section connected the two hydraulic rams, and kept them in alignment during beam loading (see Figures 1 and 2).

The connections between the top "I" beam section with the attached Enerpac™ hydraulic rams and the two supporting column sections were designed as pinned connections, following American Institute of Steel Construction (AISC) Manual of Steel Construction (92) guidelines, (Reference 4). Consequently, minimal moment reactions were developed at the connections, and only tension forces were assumed in the column sections. As a result, the end columns were designed to support a total tension load of 50,000 pounds, while keeping each column elongation less than approximately 0.1 inch. Transverse stiffeners were used on the webs of the "I" beam sections to prevent web buckling.

2.1.2 Frame Construction

As seen from Figures 1 and 2, the 20-foot long "I" beam was cut into five sections, one long section across the top, one at each base, and one short section in each column. The two 2-foot long base sections were each anchored to a 4,000 psi (compressive strength) concrete pad using six 7/8-inch diameter, 10-inch long rock bolts. The rock bolts were grouted with an epoxy resin in predrilled holes in the concrete pad. The pullout strength of each rock bolt in 4,000 psi concrete is 15,000 pounds. A twelve-inch long, 3-inch radius steel half-circular cylinder was attached to the top flange of each 2-foot long "I" beam base section, using two 1-inch diameter, 4-inch long bolts. The half-cylinders acted as beam supports during testing. The two 2-foot long "I" beam base sections with the half-cylinders were spaced on the concrete pad to obtain a simple span of 9 feet for the concrete beams. On top of each 2-foot long "I" beam
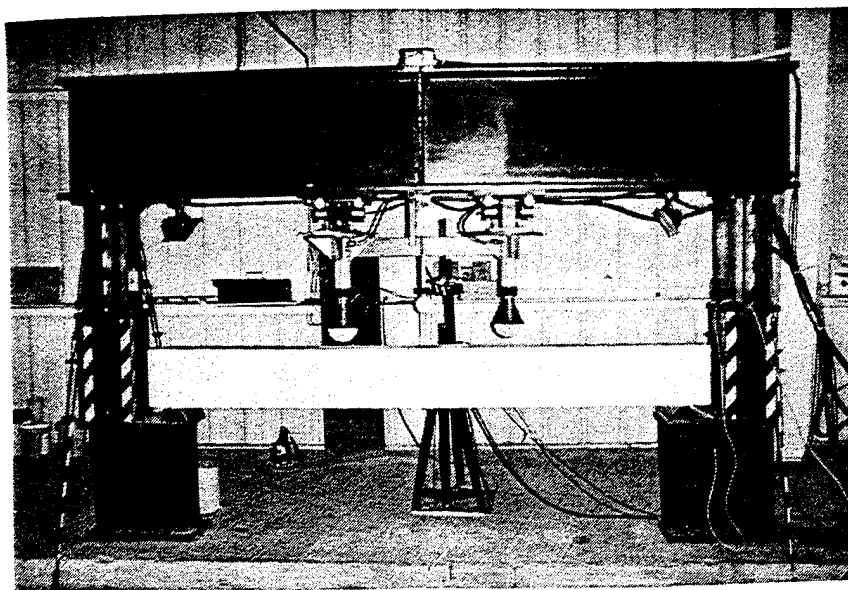
4

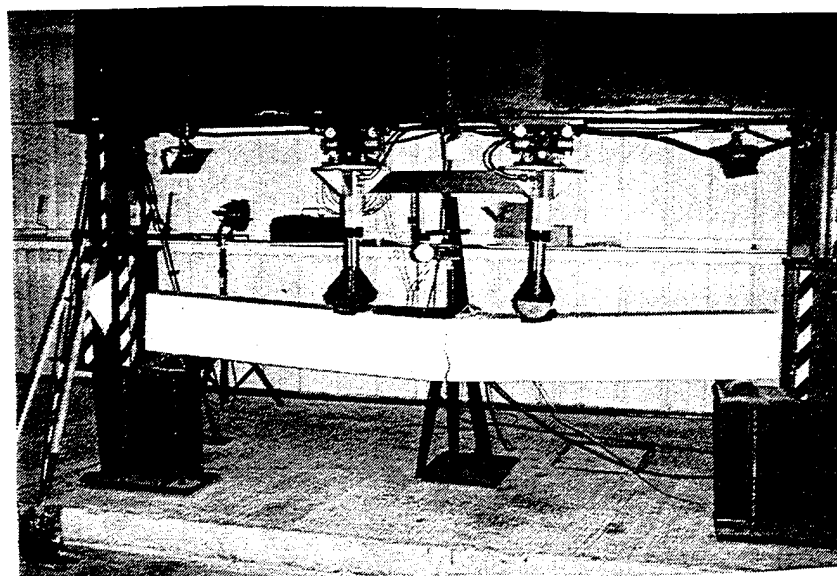Figure 1. View 1 of Load-Frame Used for Phase II Beam Testing.

Figure 2. View 2 of Load-Frame Used for Phase II Beam Testing.

base section was constructed an 11-inch square, 21-inch tall concrete box enclosed with 1/4-inch thick steel plate. The box acted as a spacer. Embedded in each concrete box were four 1-inch diameter, 20-inch long thread rods whose ends were left exposed. The rods were used to attach a 1-foot long "I" beam column section, placed on top of each box, to the 2-foot long "I" beam base section each box rested upon. The result was a 6-foot high column section. Finally, a 14-foot long "I" beam section was placed on top of the two columns sections. The overhead "I" beam was attached to each column section with four 1-inch diameter, 6-inch long bolts. Attached on the underside of the top "I" beam at the third-points of the test beam span were Enerpac™ 50,000-pound capacity hydraulic jacks. The distance between the jacks was 3 feet. Each jack was attached to the top "I" beam with four 1-inch diameter, 4-inch long bolts. A 50,000-pound capacity load cell was attached to the base of each jack. Twelve-inch long, 3-inch radius, steel half-circular cylinders were attached to the ends of each jack to act as the load points on the concrete beams. All bolts, nuts, and rods used in the construction of the load frame were manufactured from high strength steel (f_y = 60 ksi).

2.1.3   Load-Frame Operation

In general, test procedures from ASTM C 78-84, Standard Test Method for Flexural Strength of Concrete (Using Simple Beam with Third-Point Loading) and ATSM C 1018-89, Standard Test Method for Flexural Toughness and First Crack Strength of Fiber-Reinforced Concrete (Using Simple Beam with Third-Point Loading) were used to conduct the tests on and obtain load-deflection curves for each beam, (References 5,6 and 7). Flexural loading of beams used the third-point loading method. A load span to depth (L/D) ratio of 9 was used for all beams. Since the depth of all test beams was 1-foot, the load span length was set at 9 feet. To conduct a test, a 10-foot long concrete beam was placed in the load-frame on the half-cylinders attached to the two 2-foot long "I" beam base sections anchored to the concrete pad. The Enerpac™ hydraulic rams were extended using the electric pump shown in Figure 3 until the half-cylinders on the ends of the jacks came into contact with the top of the concrete beam. To test a beam to failure, one of two methods was used, depending upon whether instrumented rebar was present in the beam. If no instrumented rebar was present, the electric pump was used to slowly increase the load (3,000 to 4,000 lbs/min) on the beam through the hydraulic jacks until beam deflection reached approximately 4 to 5 inches or complete failure occurred. While the beam was being loaded, readings from a dial gage recording mid-span, top-of-beam deflection and a digital readout of the combined load cell measurements were videotaped. Later this load-deflection data was transcribed from the video using frame-by-frame advance. A view of the dial
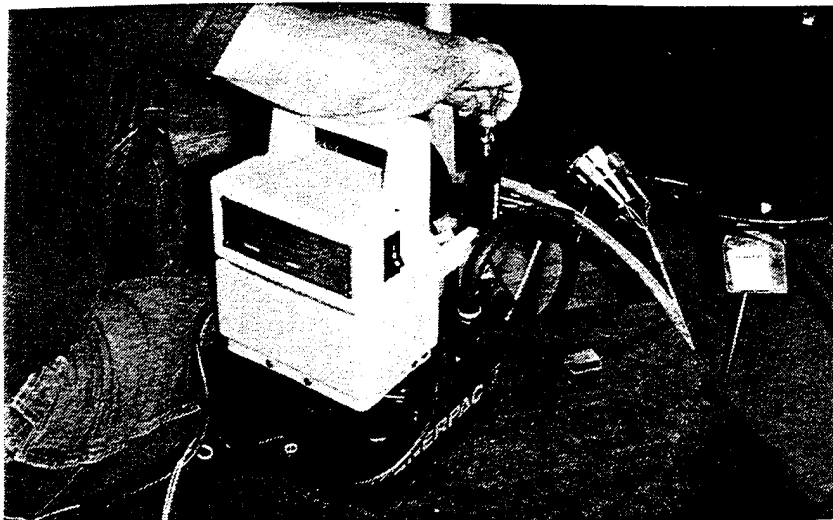
Figure 3. Electric Pump Used to Operate the Hydraulic Rams.
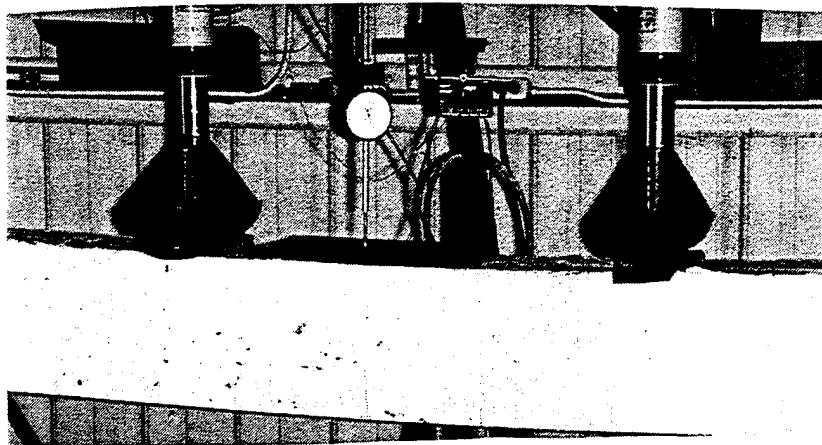
Figure 4. View of Dial Gage and Digital Readout for the Load Cells.
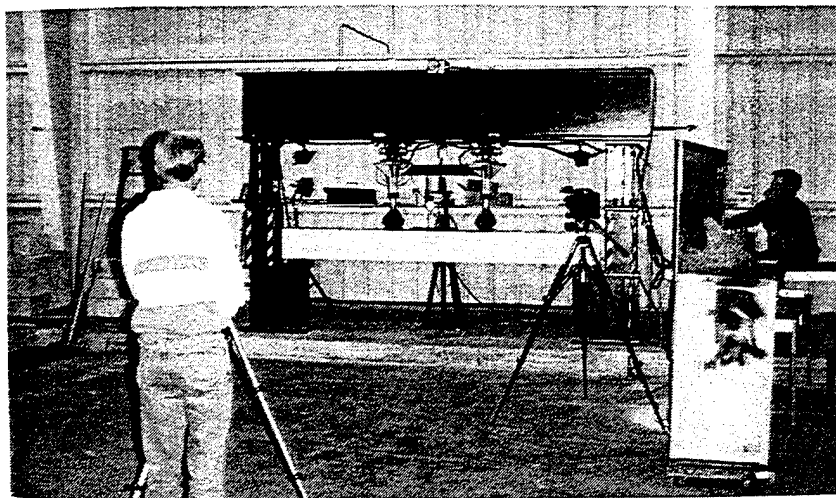
Figure 5. Video Setup to Record Dial Gage and Digital Readout Measurements.

7

gage attached to a stand placed on the concrete pad adjacent to the load-frame, with the load cell digital readout immediately to its right, is shown in Figure 4. The setup of the video equipment to record the readings from the dial gage and digital readout is shown in Figure 5.

If a beam with instrumented rebar was being tested, the loading process was paused after approximately every 1,000 pounds of applied load. The load was held, and the vibrating wire rebar strain gage data recorded using the readout box shown in Figure 6. The readout box was electrically connected to the instrumented rebar by wires cast in the beam.

2.2 TEST BEAM DESCRIPTIONS

2.2.1 Beams and Cylinders

All beam types used in the testing program are summarized in Table 1 with a corresponding Beam ID. Beam IDs given in Table 1 correspond to the Beam IDs used in Phase I testing (see Reference 3). Also included in the table are binder type, average concrete compressive strength, average concrete modulus-of-rupture, maximum concrete compressive strain at failure, amount of tension reinforcement, amount of compression reinforcement, reinforcing fiber type, percentage of fibers by volume, and average beam unit weight. Three beams were poured for each beam type. All beams were 10 feet long, 12 inches deep, and 8 inches wide. The average concrete compressive strengths shown in Table 1 come from compressive tests of 6-inch diameter, 12-inch long cylinders (3 per beam type). Maximum concrete compressive strains come from the same cylinder test data. Average modulus-of-rupture values given in Table 1 come from flexural tests of 6-inch wide, 6-inch deep, 30-inch long concrete beams (3 per beam type). Average unit weight is based on the average weight of all three beam specimens for a particular type, including fibers and rebar.

2.2.2 Fiber Types

Four different fiber types were used in the test beams. Two fiber types consisted of individual steel fibers of differing lengths and shapes, while a third type consisted of individual nylon fibers. The remaining fiber type was also steel, but in an interwoven mat matrix (see Reference 3). These fiber types were selected because they are in the most common use. In addition, they perform well at reasonable cost, and are readily available commercially worldwide. Fibers such as carbon and Kevlar® were not considered due to their high cost and limited availability. Glass fibers were not considered because of long-term durability concerns. Natural

Figure 6. Readout Box Used to Record Vibrating Wire Rebar Strain Gage Measurements.

TABLE 1. DESCRIPTIONS AND PROPERTIES OF THE TEST BEAM TYPES.

Beam ID	Binder Type(1)	Avg. Comp. Strength & Modulus of Rupture (psi)	Avg. Max. Strain (in/in)	Bars: Tension (2)	Bars: Comp. (2)	Fiber Type (3)	Fiber Vol. (%)	Avg. Unit Wt. Including Rebar (pcf)
SR4	NW/MS	7,221/1,219	0.00184	2 No. 6	2 No. 6	None	N/A	157.55
SR5	LW/HS	9,025/1,288	0.00218	2 No. 6	None	Steel-2	1.4	145.10
SR6	LW/HS	9,986/1,117	0.00265	2 No. 6	None	Steel-2 Nylon	0.93 0.50	132.90
SR8	LW/HS	8,989/1,185	0.00449	2 No. 6	None	Steel-3	2.85	136.12
M2	LW/HS	10,592/1,033	0.00359	2 No. 6	None	Steel-2 Mat	1.4 0.60	135.63

Notes: (1)   LW=Light Weight, NW=Normal Weight, HS=High Strength, And MS=Medium Strength
(2)   Standard No. 6 (6/8" Dia.) Steel Rebar, 60ksi (68.5ksi tested)
(3)   Fiber Types (see Table 2 for fiber details): Steel-2=Anchorloc; Steel-3=Short And Straight

fibers were not used because they are too weak. Fibers such as polyester and polypropylene were not considered because they provide little performance increase versus steel or nylon. For a more detailed discussion of commonly used fiber types in fiber-reinforced concrete see the literature review in Appendix A of Reference 3.

Table 2 summarizes the fiber types used in this testing program. The Fiber ID in Table 2 is the same as used in Table 1. See Table 1 for the fiber volume percentages used in each beam type.

2.2.3 Fiber-Reinforced Concrete Design Method Overview

A brief overview of the flexural design of concrete members using standard reinforcement in combination with fiber reinforcement is given below. For much more detailed discussions of this subject see References 7, 8, and 9.

Numerous design methods have been proposed for combined fiber- and rebar-reinforced concrete structural members. Some of these include the Williamson method, the Henager and Doherty method, and the Swamy and Al-Ta'an method. All of these methods are based on ACI ultimate strength design concepts. The methods differ somewhat in assumptions with regard to the strain diagram, stress block shape and depth, maximum usable strain, etc. However, each basically modifies the force diagram to account for the contribution of the fibers in the tension zone of the concrete. The ultimate moment for a singly-reinforced beam is then the sum of the couples involving the fibers in the concrete tension zone and the reinforcing bars, plus the concrete in compression.

Comparison of the different methods shows that they produce similar results (see Reference 7). However, comparison of the results from each method with experimental data shows they are overdesigned by about 15-percent. This difference is mainly attributable to the methods not taking into account the strain hardening ($\varepsilon_{steel} > \varepsilon_y$) occurring in the reinforcing steel (fibers and rebar).

In conclusion, the basic design of fiber- and rebar-reinforced concrete members does not differ significantly in method or complexity from the design of standard reinforced concrete members. Adequate methods are currently available, which, while conservative, provide reasonable accuracy. Additionally, design methods are steadily being improved. Design methods for fiber- and rebar-reinforced lightweight concrete beams will be addressed in Phase III of this research and testing effort.

TABLE 2. FIBER TYPES AND PROPERTIES.

Fiber ID	Description	Length (in)	Diameter (in)	Aspect Ratio (L/D)	Shape	Tensile Yield Strength (ksi)
Steel-2	Anchorloc Steel Fibers By Mitchell Fibercon, Inc. Twisted Shape	1.0	0.10 x 0.044	42	⌇	60
Steel-3	Short Steel Fibers By MeH-Tec	0.625	0.020	32.25	—	100
Nylon	Nylon 6 By NyCon, Inc.	1.0	0.0009	111.11	——	130
Mat	Steel Fiber Mat By Ribbon Technology	N/A	N/A	N/A	See Reference 1	N/A
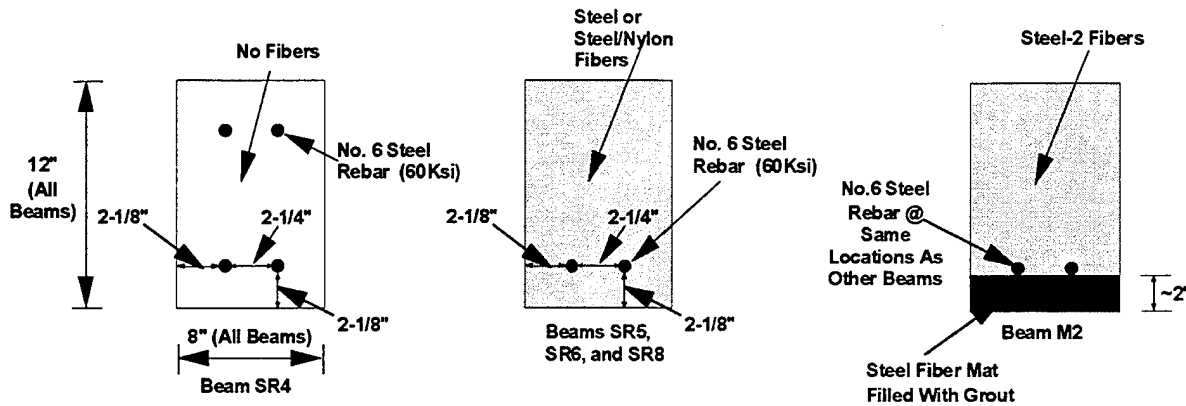
Figure 7. Test Beam Cross-Sections.

TABLE 3. BEAM REINFORCING PARAMETERS.

Beam ID	b (in)	d (in)	A_s (in²)	ρ_b	ρ_{max}	ρ	ρ/ρ_b	ρ/ρ_{max}	ACI Ultimate Moment (in-kips)(2) & Total Load (3) (kips)
SR4(1)	8.0	9.5	0.88	0.0277	0.0208	0.0116	0.4188	0.5577	536.5/29.8
SR5	8.0	9.5	0.88	0.0354	0.0266	0.0116	0.3277	0.4361	543.9/30.2
SR6	8.0	9.5	0.88	0.0432	0.0324	0.0116	0.2685	0.3580	546.8/30.4
SR8	8.0	9.5	0.88	0.0482	0.0361	0.0116	0.2407	0.3213	543.8/30.2
M2	8.0	9.5	0.88	0.0522	0.0392	0.0116	0.2222	0.2959	548.3/30.5

Note: (1) Double reinforcing parameters for this beam type are: $A_s' = 1.32$ in², $d' = 2.5$ in, and $\rho' = 0.0174$

(2) $M_n = \rho f_y b d^2 (1 - \beta \rho\, f_y / f_c'\, \alpha)$ Where: M_n = Ultimate Moment Capacity, A_s = Tension Steel Area, f_y = Tension Steel Yield Strength, d = Depth to Centroid of Tension Steel, ρ = Reinforcement Ratio, f_c' = Concrete Compressive Strength, b = Beam Width, and α and β = concrete strength factors

(3) Ultimate moment divided by third-point distance then multiplied by 2 ((M$_u$ / 36") x 2)

11

2.2.4   Beam Standard Reinforcing Parameters

Standard Number 6 steel rebar (3/4-inch diameter, 60 ksi yield strength, 29,000,000 psi modulus of elasticity, and unit weight of 1.502 lbs per linear foot) was used in all beam types. The Number 6 rebar stock used to fabricate the beams was tested, and the rebar's actual yield strength was determined to be 68.5 ksi.

A total of three test beam cross-sections, with and without vibrating wire rebar strain gages, were used in the test program. These beam cross-sections are shown in Figure 7. Stirrups were used only in the control beams (beam type SR4), which also had Number 6 rebar in the compression zone, so that the beams were symmetrically reinforced. The control beams also used standard weight concrete instead of lightweight concrete. The locations of rebar reinforcement are shown on the beam cross-sections in Figure 7. More information on standard rebar reinforcing parameters is given below.

2.2.4.1   Singly Reinforced Beam Types

For the singly reinforced beam types (SR5, SR6, SR8, and M2), the balanced reinforcing ratio, ρ_b, was determined using the American Concrete Institute (ACI) equation shown below (Reference 10):

$$\rho_b = \frac{\alpha f_c'}{f_y} \left(\frac{E_s \varepsilon_c}{E_s \varepsilon_c + f_y} \right)$$ (1)

Where: $\rho = A_s / bd$

ρ_b = Value of ρ at which the reinforcing steel yields at the same time as the concrete in the compression zone crushes

ε_c = Extreme fiber concrete compressive strain at which crushing is assumed to occur

f_y = Steel tensile yield strength (68.5 ksi)

E_s = Steel modulus of elasticity (29,000,000 psi)

f_c' = Concrete cylinder compressive strength (see Table 1)

α = Average compressive stress in the concrete compression zone at crushing, divided by f_c' (for $f_c' > 8,000$ psi α=0.56 and for f_c'=6,000 to 7,000 psi α=0.64)

The values for α given above were developed by the ACI for concrete without fiber reinforcement. However, using these α values in the design of fiber-reinforced concrete members provides sufficient accuracy according to References 7, 8, 9, and 11. The maximum allowable ACI reinforcing ratio was determined using $\rho_{max} = 0.75\rho_b$. The actual reinforcing ratio for each beam was determined using $\rho = A_s / bd$, where A_s is the reinforcing steel area, b = beam width, and d = depth to the centroid of tension reinforcement. The average

reinforcing parameters for all singly reinforced beam types are summarized in Table 3. As seen from Table 3, all beam types are under-reinforced. Table 3 also contains the ACI ultimate moment capacity for each beam type, along with the total load (two times the individual hydraulic ram loads) needed to reach the specified moment capacity.

2.2.4.2 Doubly Reinforced Beam Types

For the doubly reinforced beam type (control beams, type SR4), the balanced reinforcing ratio (ρ_b) was determined using Equation (1) above. Then, as before, the allowable ACI reinforcing ratio and the actual reinforcing ratio were determined using $\rho_{max} = 0.75\rho_b$ and $\rho = A_s / bd$, respectively. According to the ACI, if ρ is equal to or less than ρ_{max}, a doubly reinforced beam may be designed with acceptable accuracy by ignoring the compression reinforcement and designing the beam as a singly reinforced beam. Since ρ_{max} was greater than ρ (0.0208 versus 0.0116) for the SR4 beam type, the SR4 doubly reinforced beams were treated as singly reinforced. If this had not been the case, the ACI equations given below would have been used to calculate beam reinforcing parameters so that both tensile and compressive steel reinforcing will yield by the time the concrete crushes.

$$\rho' = \frac{A'_s}{bd} \tag{2}$$

$$\bar{\rho}_{max} = 0.75\rho_b + \rho' \tag{3}$$

$$\bar{\rho}_{lim} = 0.85\beta_1 \frac{f'_c}{f_y} \frac{d'}{d} \frac{\varepsilon_u}{\varepsilon_u - \varepsilon_y} + \rho' \tag{4}$$

Where: A'_s = Compression steel area

$\beta_1 = 0.65$ for $f'_c \geq 8,000$ psi

d' = Depth to centroid of compression reinforcing steel

$\varepsilon_u = 0.00184$ (see Table 1, SR4 beam type average concrete cylinder test data)

$\varepsilon_y = 0.00236$ (f_y/E_s, i.e., 68.5 ksi / 29,000 ksi)

ρ' = Compression steel reinforcing ratio

$\bar{\rho}_{max}$ = Maximum allowable tensile steel reinforcing ratio

$\bar{\rho}_{lim}$ = Minimum allowable tensile steel reinforcing ratio

2.2.5 Beam Fabrication and Mixture Properties

Three concrete forms of the appropriate dimensions were fabricated out of lumber. Holes were drilled through the ends of the forms, allowing rebar to be preplaced in the forms prior to pouring concrete. The holes were drilled at appropriate locations to obtain the reinforcement dimensions shown in Figure 7.

13

A small, towable, 1 cubic yard capacity concrete mixer was used to mix the concrete. Fibers, if used, were added toward the end of the mixing process. The concrete was mixed for approximately 10 to 15 minutes, then poured into the forms. A pencil, internal vibrator and attachable form vibrators were used to consolidate the concrete in the forms. After consolidation, the exposed concrete surface was finished with trowels. The forms were then covered with wet burlap for approximately 24 hours. The beams were then removed from the forms, and recovered with wet burlap. During the remaining 27 day curing time, the burlap covering the beams was continuously wetted with a water sprinkler. Views of the beam fabrication process are shown in Figures 8 and 9.

Concrete from the same batch was poured into 6-inch diameter, 12-inch long concrete cylinder forms and 6-inch wide, 6-inch deep, 30-inch long beam forms. After 24 hours, the cylinders and beams were removed from the forms and cured under water for 27 days. The cylinders were used to obtain concrete compressive strength and maximum compressive strain data for each concrete mix. The beams were used to obtain modulus-of-rupture values for the concrete mixes. Mix designs for the different concretes used in the beam types are given in Table 4. A Type-1 cement was used in all mixes.

In addition to the concrete mixes described in Table 4, a slurry mixture consisting of 55 pounds of Type-3 cement, 13.5 pounds of water, 450 grams of polymer modifier (Tylac 97-314), 130 grams of a water reducer (WRDA-79), 65 grams of a superplasticizer (WRDA-19), and 50 grams of a retarder (WRDA-17) was used for test beam type M2. The slurry was used to infiltrate the steel fiber mat matrix. The steel-fiber mat matrix was preplaced in the bottom of the concrete forms prior to infiltration. After slurry infiltration, concrete was poured over the infiltrated steel mat to complete the beams.

2.2.6   Compressive Cylinder Tests

Compressive tests of 6-inch diameter, 12-inch long concrete cylinders poured at the same time individual beams were poured were done using a 500,000-pound capacity Forney load-frame under load control, following the procedures given in ASTM C 39, Standard Test Method for Compressive Strength of Cylindrical Concrete Specimens, (Reference 12). Average compressive strength and maximum concrete strain results from these cylinder tests are given in Table 1.

In addition to the concrete cylinder test outlined above, 4-inch diameter, 8-inch long cores were taken from the unstressed ends of beams after testing was completed. The cores were also tested on the Forney to determine concrete compressive strength. Results from these tests are presented in Table 5. As seen from Table 5, these compressive strength results agree quite well with the strength results given in Table 1. In fact, the average concrete compressive

14

strengths given in Table 5 are slightly higher than those given in Table 1. This discrepancy is probably caused by the smaller cylinder size for the results given in Table 5, which tends to increase compressive strength results. Still, comparison of the concrete compressive strength results given in Tables 1 and 5 indicate quality control was good during the beam fabrication process. It does not appear that any mix separation or fiber balling occurred. If such things had occurred there would probably have been a greater variance between compressive strength results given in the two tables.
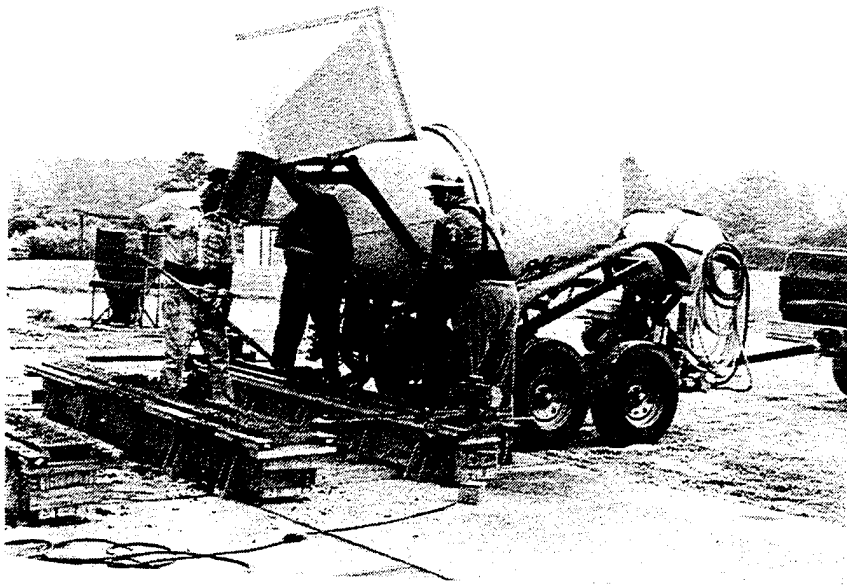
Figure 8. View 1 of the Beam Fabrication Process.
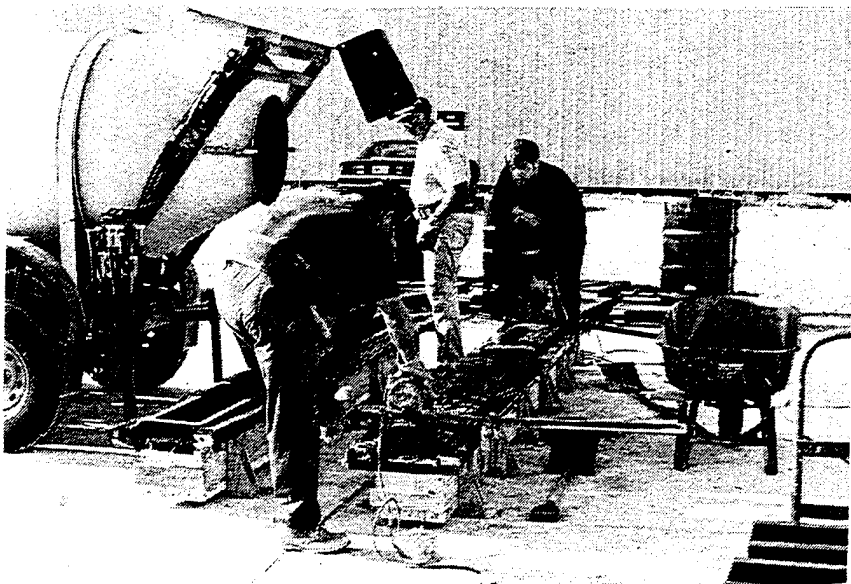
Figure 9. View 2 of the Beam Fabrication Process.

TABLE 4. CONCRETE MIX DESIGNS FOR TEST BEAMS, BASED ON 1 YEAR.

Beam ID	Fibers (lbs) (1)	Cement (lbs)	Fine Agg. & Sand (lbs)	Coarse Agg. (lbs)	Solite (lbs) (2)	F-10K (lbs) (3)	Water (lbs) & Water/Cement Ratio (w/c)	WRDA -79 (oz) (4)	WRDA -19 (oz) (5)	Slump (in)	Unit Weight (pcf)
SR4	None	812	1,100 29.5	1,750	N/A	N/A	342 w/c: 0.42	N/A	N/A	3	151
SR5	190 (S2)	940	1,230 87.3	N/A	850	218	214 w/c: 0.23	50	60	3	142.1
SR6	124 (S2) 10 (N)	940	1,230 50	N/A	850	218	214 w/c: 0.23	50	60	4	132.9
SR8	380 (S3)	940	1,230 31	N/A	850	218	214 w/c: 0.23	50	60	3	133.0
M2	190 (S2)	940	1,230 11	N/A	850	218	214 w/c: 0.23	50	60	5	129.8

Notes: (1) N=Nylon, S2= Steel-2, and S3= Steel-3
(2) Lightweight aggregate
(3) Force-10K liquid silica flume by W. R. Grace, Co.
(4) Water reducer by W. R. Grace, Co.
(5) Super plasticizer by W. R. Grace, Co.

TABLE 5. 4- BY 8-INCH CONCRETE CYLINDER COMPRESSIVE STRENGTHS.

Beam Type	Core 1 Comp. Strength (psi)	Core 2 Comp. Strength (psi)	Core 3 Comp. Strength (psi)	Core 4 Comp. Strength (psi)	Core 5 Comp. Strength (psi)	Core 6 Comp. Strength (psi)	Average Comp. Strength (psi)
SR4	6,564	7,744	8,088	8,289	8,740	7,910	7,889
SR5	9,600	10,080	11,165	9,415	N/A	N/A	10,065
SR6	11,138	11,126	11,119	10,870	10,361	11,200	10,969
SR8	11,327	10,994	10,277	9,723	13,317	13,322	11,493
M2	7,765	11,702	10,614	10,245	9,819	12,449	10,432

SECTION 3

TEST RESULTS -- INSTRUMENTED REBAR BEAMS

3.1 INSTRUMENTED REBAR CONFIGURATION

As previously indicated, two out of the three beams of each beam type were instrumented with vibrating wire rebar strain gages. The gages were recessed in a 3-foot section of Number 6 rebar. The vibrating wire strain gage, which was covered by a plastic sleeve, was recessed in the middle 6 inches of the rebar section. A 30-foot long wire, through which gage data was recorded during testing, was attached to the middle of the gage. The diameter of the entire gage was the same as that of the rebar. Standard Number 6 rebar sections were welded on both ends of the instrumented rebar section to obtain an overall length of 10.25 feet. This composite rebar section was then placed in a concrete form and cast in place. The recording wire for the gage was positioned so it passed out the top of the beam. The wire was attached to the readout box (see Figure 6) to record strain during testing.

In the SR5, SR6, SR8, and M2 beam types, one instrumented rebar was used per beam. The instrumented rebar was the tension rebar closest to the beam side facing the video camera used to record deflection and load during testing (see Figure 5). For the SR4 beam type, which used both tension and compression rebar reinforcement, two instrumented rebars were used per beam. The instrumented rebar in an SR4 beam's tension zone was located in the same position as it was in the other four beam types. The rebar in the compression zone was located diagonally opposite the tension rebar.

3.2 TEST RESULTS

3.2.1 Load-Deflection Curves

A total of five beam types were tested (two instrumented rebar beams per type). SR5, SR6, and SR8 beam types were reinforced with steel rebar in the tension zone and various types of fiber reinforcement. No stirrups were used in these beam types. The SR4 beam type, which acted as the control, representing current hardened structure construction practice, i.e. standard weight concrete, symmetrically rebar-reinforced with stirrup shear reinforcement, had two Number 6 rebars in both the tension and compression zones. A total of eight Number 3 rebar stirrups were used for each half of an SR4 beam (total of 16 per beam). For each beam half, the first stirrup was placed 3 inches from the end of the beam, with the next spaced 6 inches from the

18

first. The next six stirrups were spaced at 7-inch intervals. The M2 type beams were reinforced at the bottom with the slurry-infiltrated steel fiber mat, with steel fiber-reinforced concrete above the mat. In addition, the M2 beam type also had two Number 6 rebars in the tension zone.

The beams were tested on the load-frame shown in Figures 1 and 2 to generate load-deflection curves for each beam type. The load-deflection curves for beams 1 and 2 of each beam type are given in Figures 10 and 11, respectively. These curves show total load versus mid-span, top-of-beam deflection for each beam type. No curve for SR5 beam 2 is shown in Figure 11 because this beam cracked during transportation to the test site. Also in Figure 11, the curve for SR6 beam 2 terminates prematurely because the batteries powering the video cameras collecting load-deflection data failed part way through the test. Typical views of the instrumented beam testing process are shown in Figures 12 to 15.

3.2.2   Instrumented Rebar Results

Tension strain gage measurements as a function of total beam load for beams 1 and 2 of each beam type are shown in Figures 16 and 17, respectively. Readings from the gages in the compression zone of beams 1 and 2 of beam type SR4 are presented in Figure 18. For the reasons given in the preceding subsection, strain-load curves for beam 2 of beam types SR5 and SR6 are not shown on Figure 17.

While there is some variance in the strain-load curves presented in Figure 16 and 17, the differences are not significant nor consistent enough to make any conclusions regarding whether the different concrete matrices influenced the behavior of the reinforcing rebar. A more thorough test regimen, with enough beams to yield statistically significant data, would be required to determine whether the different concrete matrices influenced the behavior of the rebar. Such a test regimen is desirable because there is enough variance in the rebar strain-load curves given in Figures 16 and 17 to suggest that the concrete matrices may have influenced the behavior of the embedded rebar.

3.2.3   Beam Failure Mode

One major observation resulting from the testing of instrumented rebar beams was that the instrumented rebar had a direct effect on the failure mode of the beams. A plastic sleeve was used to cover the vibrating wire strain gage in an instrumented rebar. Thus, no bonding could occur between the concrete and rebar at the location of the sleeve on an instrumented rebar. During testing, a large crack developed in the concrete at the location of the sleeve in the
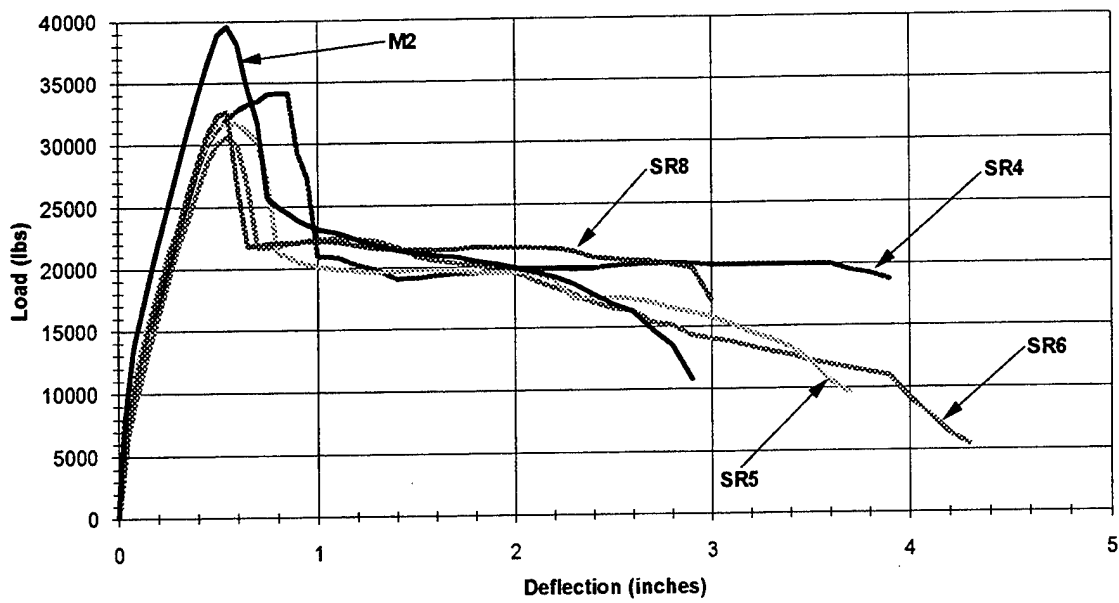
Figure 10. Load-Deflection Curves, Beam 1 (Instrumented Rebar).
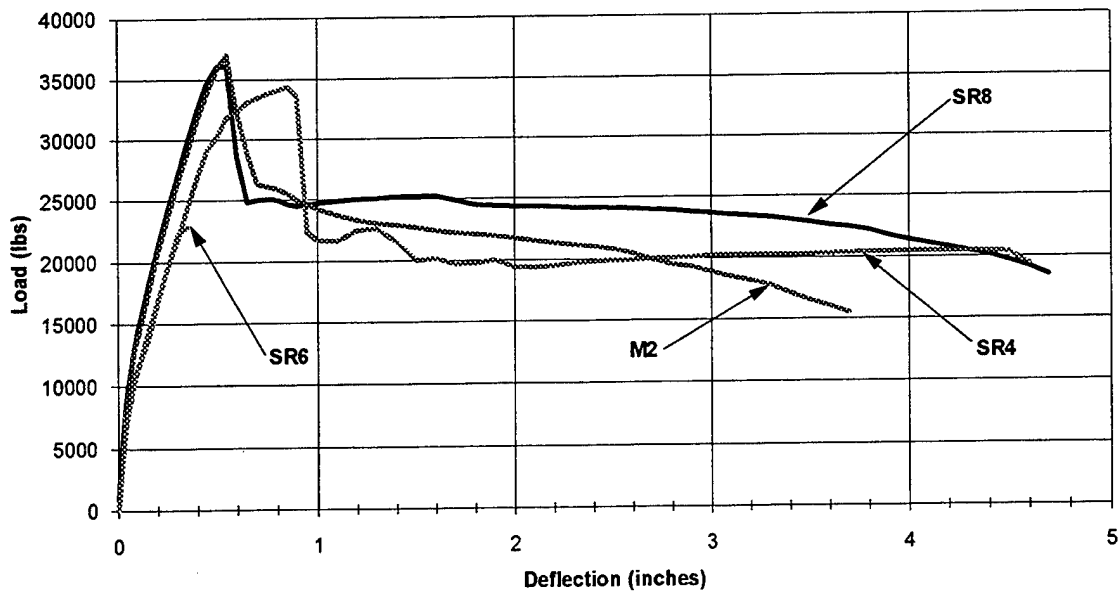
Figure 11. Load-Deflection Curves, Beam 2 (Instrumented Rebar).

20

Figure 12. View 1 of the Instrumented Rebar Beam Testing Process.

Figure 13. View 2 of the Instrumented Rebar Beam Testing Process.

Figure 14. View 3 of the Instrumented Rebar Beam Testing Process.

Figure 15. View 4 of the Instrumented Rebar Beam Testing Process.
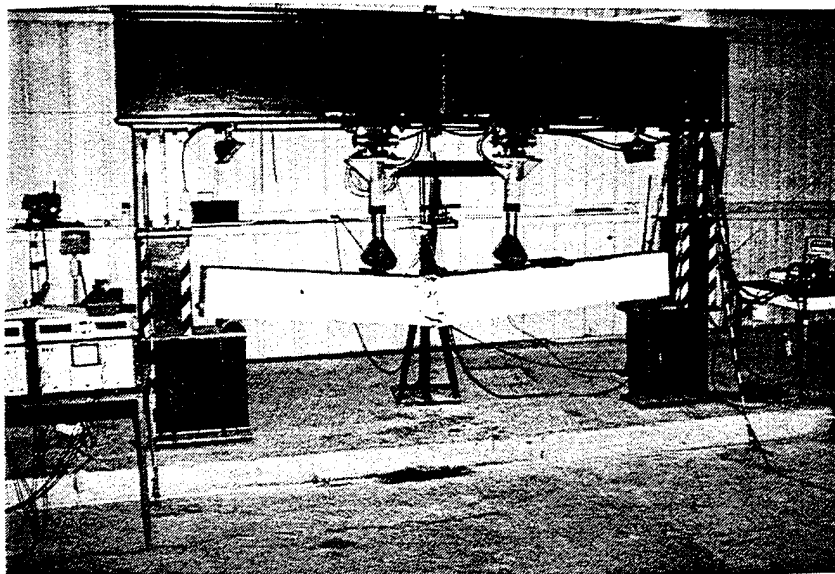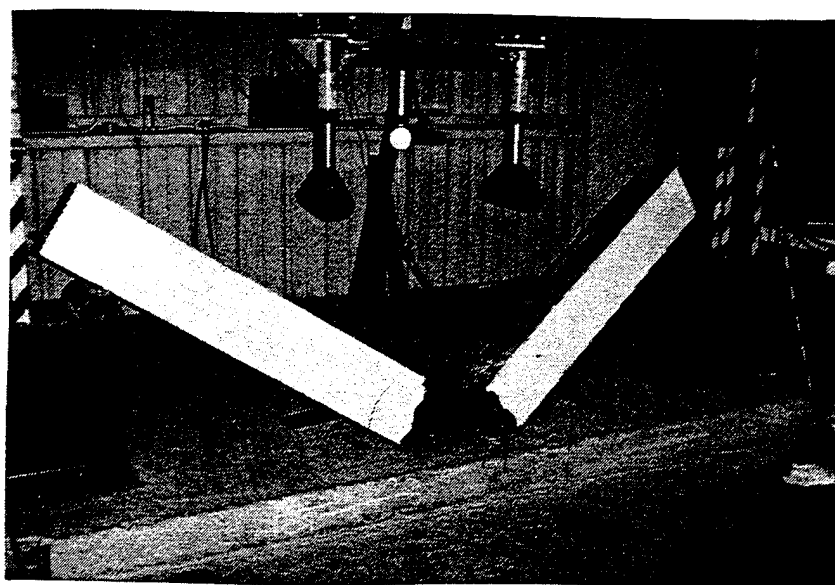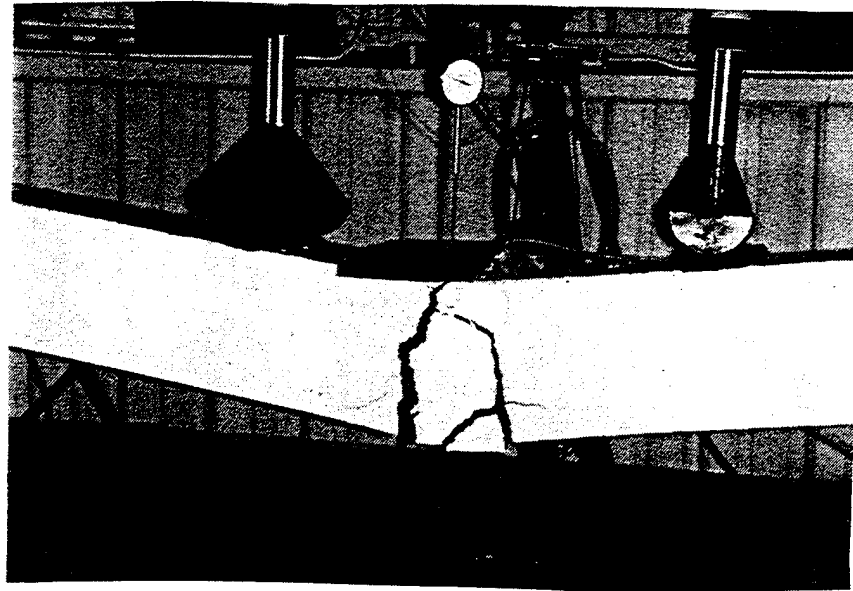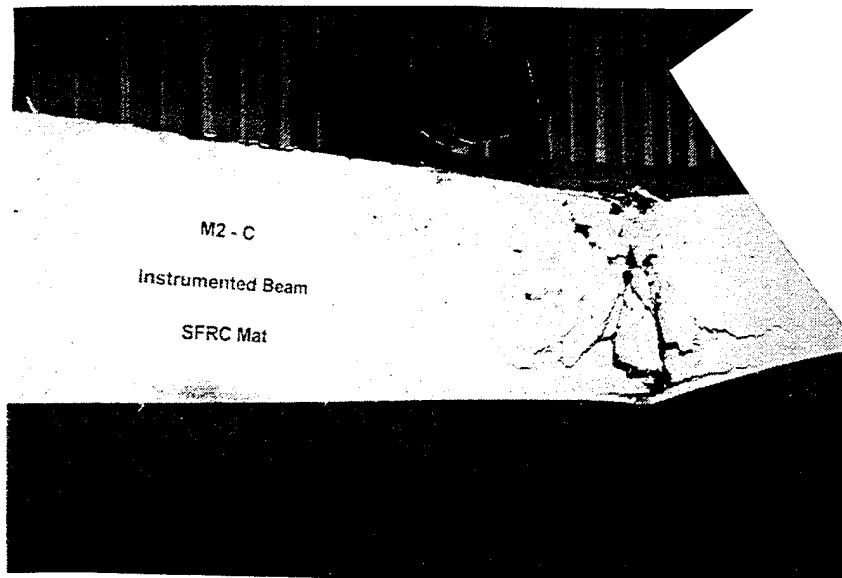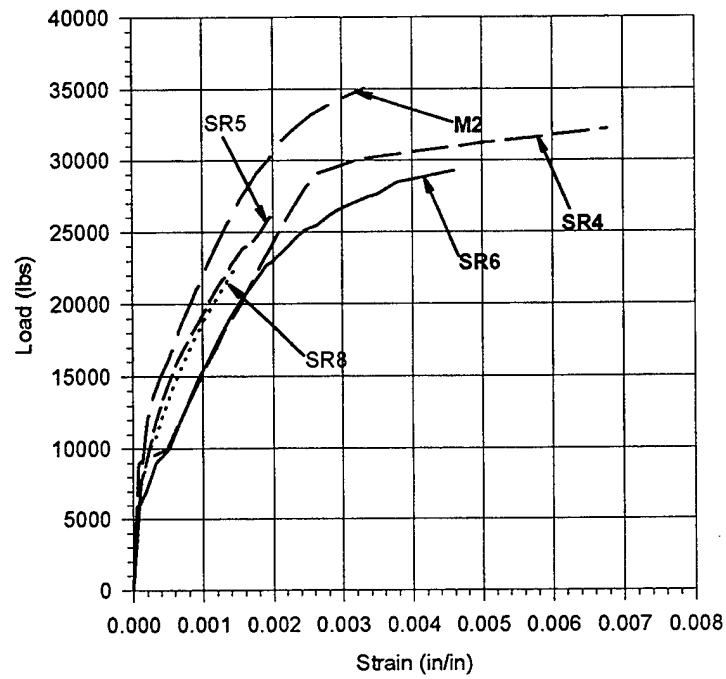
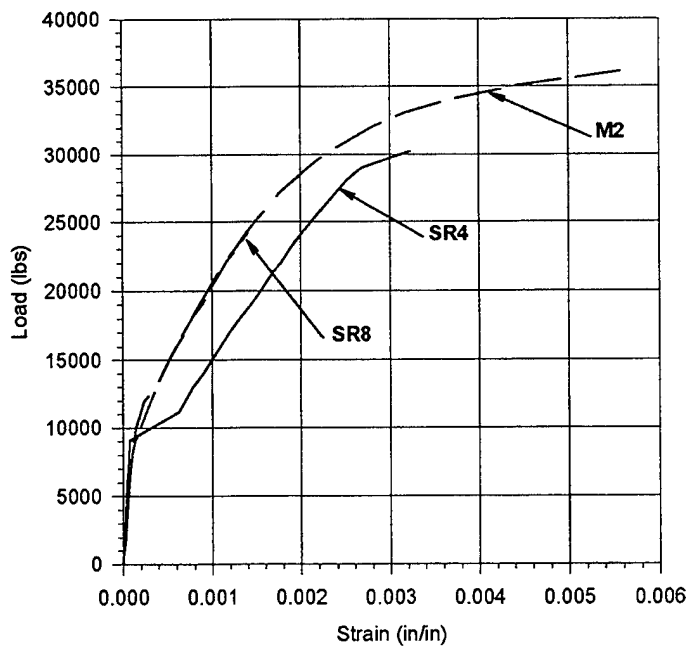Figure 16. Strain-Load Curves, Beam 1 (Instrumented Rebar).

Figure 17. Strain-Load Curves, Beam 2 (Instrumented Rebar).
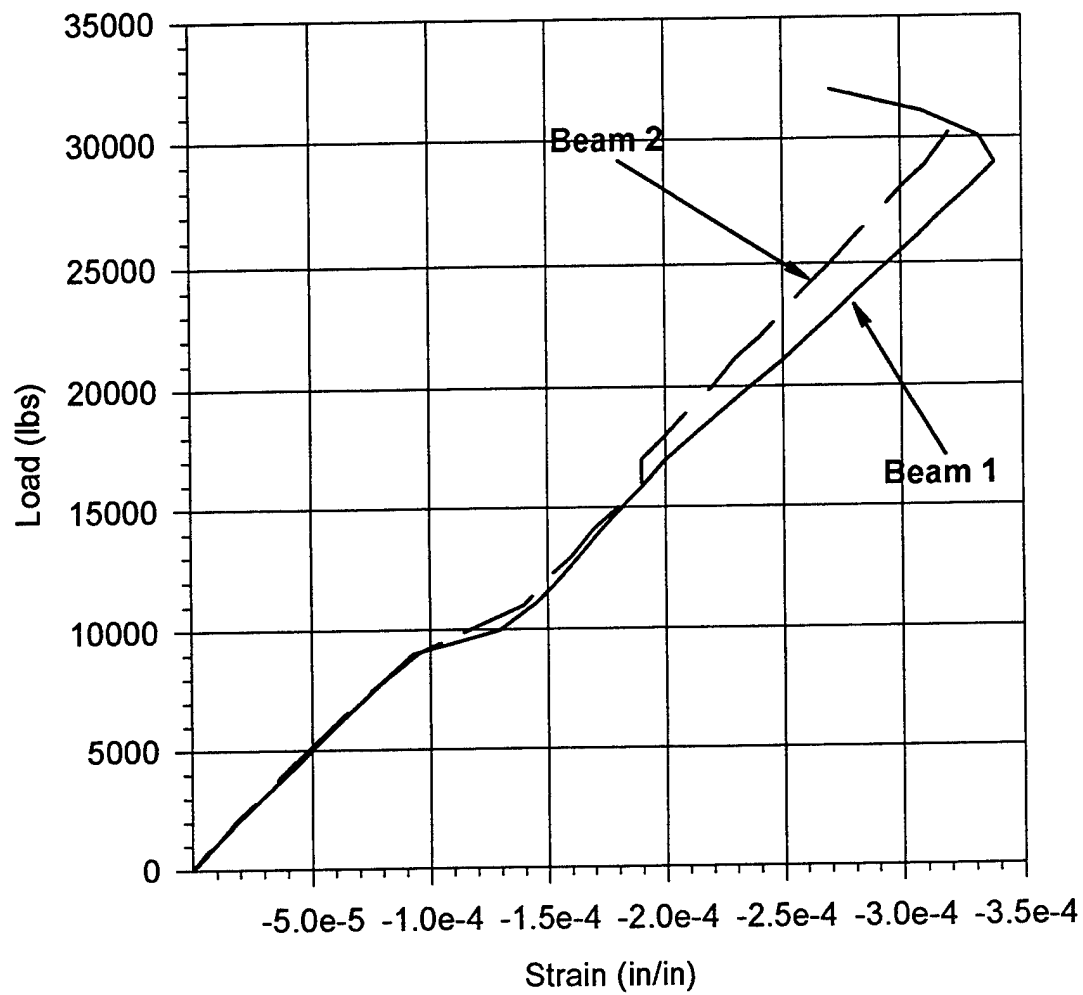
23

Figure 18. Strain-Load Curves, Beam Type SR4 (Compression Zone).

instrumented beams. The crack location corresponded roughly to the middle of the tension zone between the two load points. Very little cracking was observed in the rest of the tension zone. In the beams without the instrumented rebar, distributed cracking was observed throughout the tension zone between the two load points (See Section IV). Because the entire tension zone between the load points was not utilized to support the applied load, the capacity of the instrumented beams was in general less than that of the non-instrumented beams.

Two examples of this large crack failure mode are shown in Figures 19 and 20 for one beam and Figures 21 and 22 for another. A close up of a large crack caused by instrumented rebar is shown in Figure 23. The instrumented rebar can be seen in the crack.

3.2.4 Ductility Indices and Energy Ratios

The performance of the various beam types was compared using ductility indices and energy ratios. In addition, the average total energy absorbed by a beam type, measured in inch-pounds, i.e. the total area under a load-deflection curve, divided by the average weight of the beam type in pounds, was also used to compare the beams. The method used to calculate ductility indices and energy ratios from load-deflection curves is shown in Figure 24. This method for concrete beams was obtained from Reference 13, where it is described in detail.

As shown in Figure 24, the maximum load P_{max} is determined. Then, a straight line is drawn parallel to the deflection axis until it intersects the load axis. Next, a secant is drawn from the origin through the point on the load-deflection curve corresponding to $0.75P_{max}$, and extended until it intersects the straight line running from P_{max} to the load axis. At this intersection point, a vertical line parallel to the load axis is drawn until it intersects the deflection axis. The point where this line intersects the deflection axis (Δy) is considered the yield deflection for the beam. The energy dissipated at yield (Ey) is defined as the shaded area under the load-deflection curve up to the yield deflection as shown in Figure 24. Next, the ultimate deflection point of the curve (Δu) is determined, and the total area under the load-deflection curve up to this point (Eu) is calculated. In this test phase, ultimate deflections ranged from 2.6 to almost 5 inches. The ductility index is defined as the ultimate deflection divided by the yield deflection ($\Delta u/\Delta y$), while the energy ratio is defined as the ultimate area divided by the yield area (Eu/Ey).

3.2.5 Beam Test Results

Using the methods described in Subsection 3.2.4, ductility indices, energy ratios, and total absorbed energy per pound were calculated for each beam. The beam span, 9 feet, was used to calculate beam weight for absorbed energy per pound calculations. Results of all these calculations are given in Table 6.

Figure 19. View 1 of Large Crack Failure Mode Caused By Instrumented Rebar, Example 1.

Figure 20. View 2 of Large Crack Failure Mode Caused By Instrumented Rebar, Example 1.
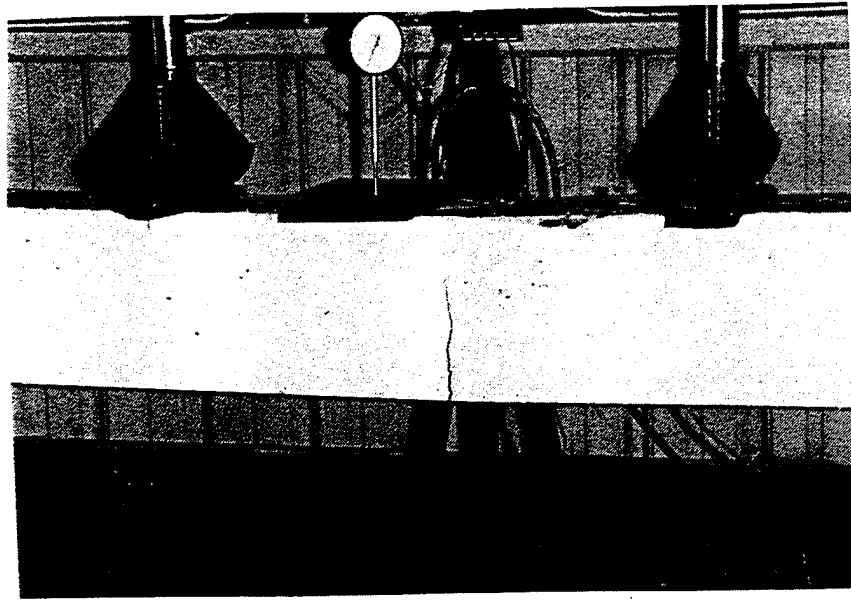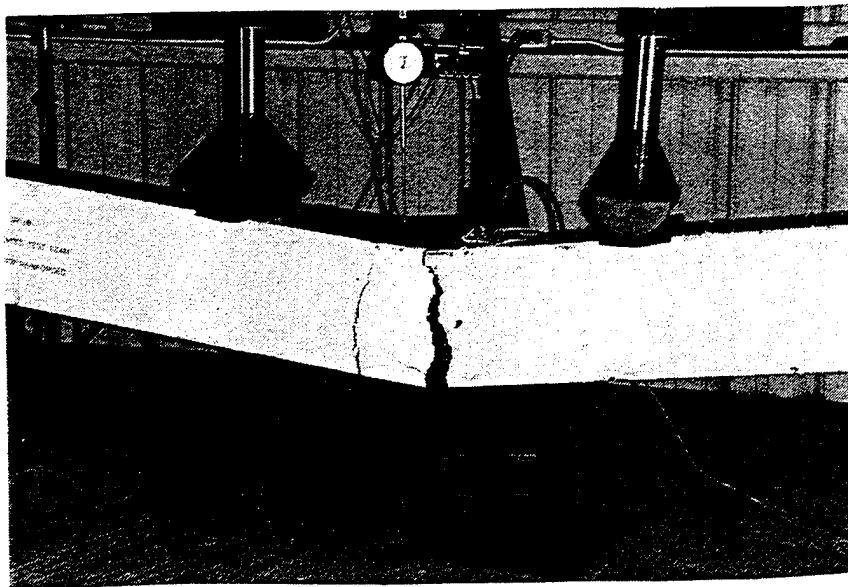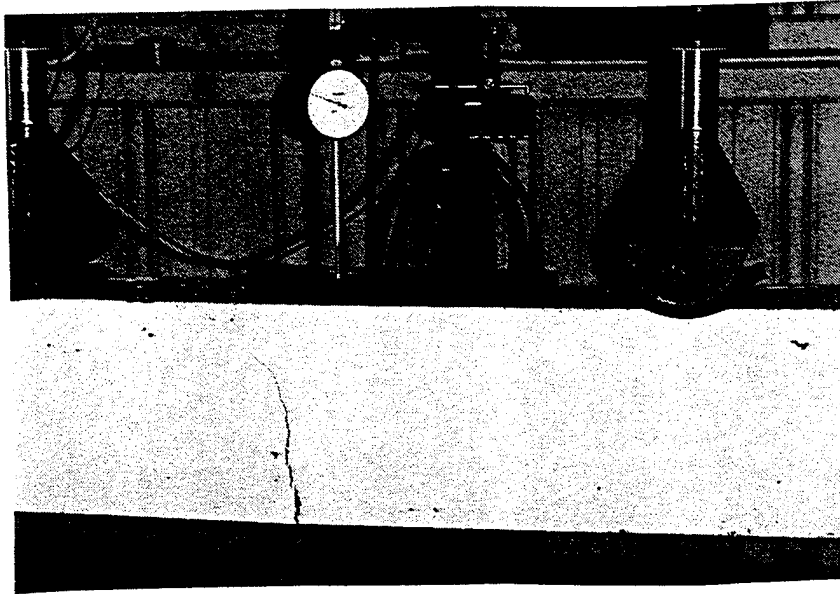
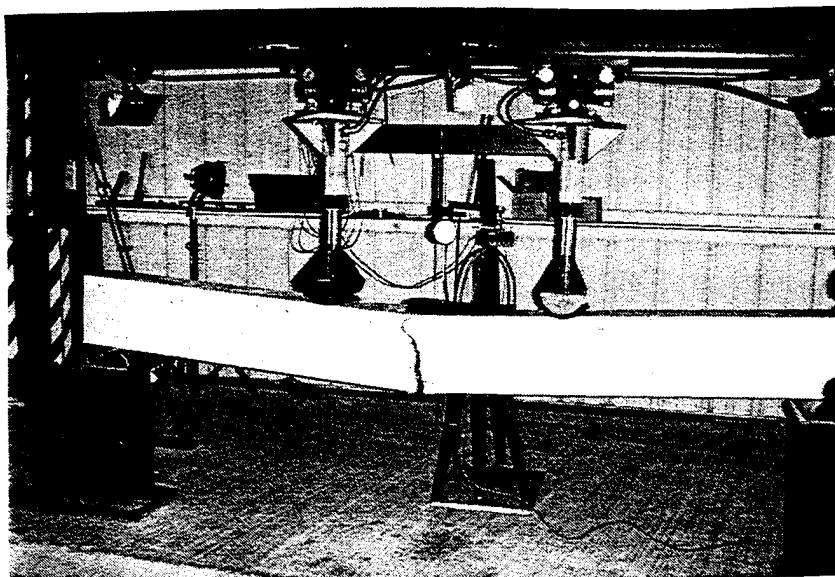Figure 21. View 1 of Large Crack Failure Mode Caused By Instrumented Rebar, Example 2.

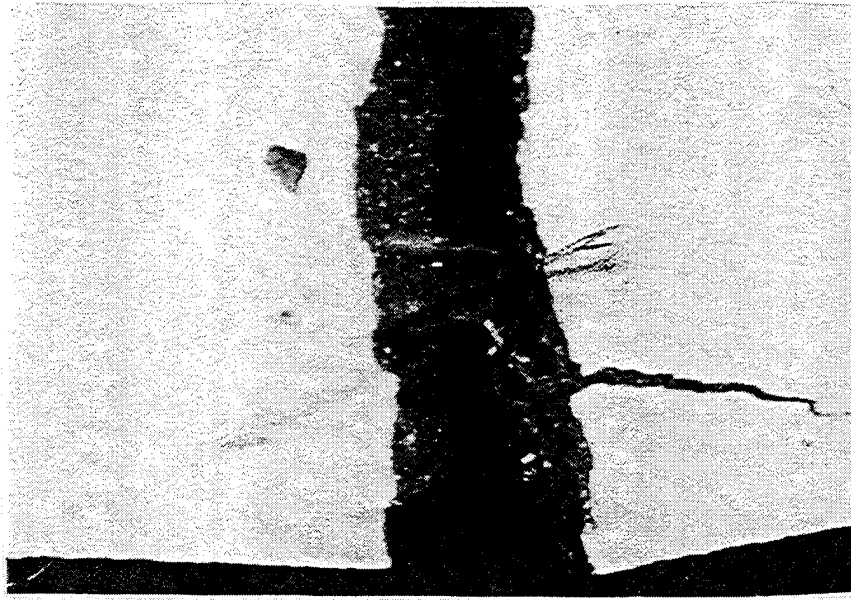Figure 22. View 2 of Large Crack Failure Mode Caused By Instrumented Rebar, Example 2.

Figure 23. Close-up of a Large Crack Caused By Instrumented Rebar.
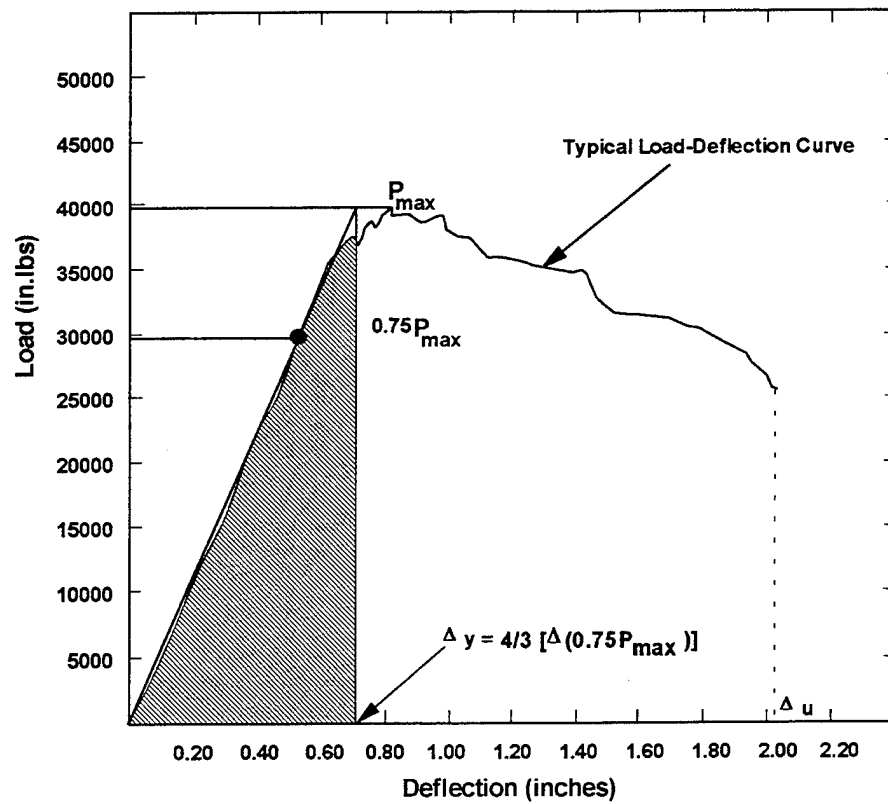

Figure 24. Calculation of Ductility Index and Energy Ratio From A Load-Deflection Curve.

28

On the basis of the results given in Table 6, each beam type was ranked by average ductility index, energy ratio, maximum load, and energy absorption per pound. This information is presented in Table 7. On the basis of these rankings, the beam types providing the best overall performance can be quickly determined and outstanding performance by a beam type in any particular area easily identified.

In addition to the results presented in Table 7, average ductility index, energy ratio, and energy absorption per pound were normalized with respect to the baseline beam type SR4. This information is presented in Table 8. This information allows the beam types providing the best overall performance versus what is currently used in hardened structure construction to be readily identified.

As shown in Tables 6 and 7, several beam types show good results. Beam type SR8 is the highest rated for average energy ratio and energy absorption per pound. In addition, beam type SR8 is rated second for average maximum load. Its worst finish is third for average ductility index. Beam type M2 is the highest rated for average ductility index and average maximum load. In addition, beam type M2 is rated second for energy absorption per pound. Its worst finish is third for average energy ratio. Beam type SR6 is rated second for average ductility index and energy ratio. However, it appears near or at the bottom of the remaining two categories. Beam type SR5 does not rate well, finishing last or second to last in all 4 categories.

For prefabricated, modular, rapidly erectable hardened shelters, where overall energy absorption and ductility as a function of weight are critical, beam types SR8 and M2 offer the best overall performance. Beam type M2 provides the highest maximum load and ductility ratio values, while beam type SR8 provides the highest energy absorption and energy ratio values.

Table 8 presents two facts. First, the beam types that show good performance, based on Tables 6 and 7, also show good performance when normalized against the baseline beam type SR4. Second, only the SR5 and SR6 beam types fail to exceed the SR4 beam type's performance level in all categories. Specifically, beam type SR5 provides inferior energy ratio and energy absorption values, while beam type SR6 provides inferior energy absorption.

Beam test results discussed above were certainly influenced by the large crack beam failure mode caused by the instrumented rebar (see Subsection 3.2.3). However, the effects of the failure should be uniform throughout the beam types. Consequently, the relative performance of the beams should be unchanged. However, if factors such as lightweight concrete and/or lack of stirrup shear reinforcement caused the influence of the large crack failure mode to increase, the good performance of the SR8 and M2 beam types is all the more gratifying. Whether this is the case will be clearer when non-instrumented beam test results are discussed in Section IV.

TABLE 6. DUCTILITY INDICES, ENERGY RATIOS, AND ABSORBED ENERGY PER POUND FOR TEST BEAMS (INSTRUMENTED).

Beam ID	Beam No.	Yield Deflc. (in)	Max. Deflc. (in)	Duct. Index	Avg. Duct. Index	Yield Area (in.lbs)	Ult. Area (in.lbs)	Energy Ratio	Avg. Energy Ratio	Max. Load (lbs)	Avg. Max. Load (lbs)	Energy (in.lbs) Per lb (1)
SR4	1	0.47	3.90	8.30		2,784	81,139	29.14		34,110		
	2	0.52	4.48	8.61	8.46	2,647	92,221	34.84	31.99	34,366	34,238	92.00
SR5	1	0.38	3.57	9.39		2,186	69,402	31.75		31,669		
	2(2)	—	—	—	9.39	—	—	—	31.75	—	31,669	79.72
SR6	1	0.38	4.25	11.18		1,897	69,055	36.40		30,594		
	2(3)	—	—	—	11.18	—	—	—	36.40	—	30,594	86.60
SR8	1	0.40	3.20	8.00		2,149	71,988	33.50		37,988		
	2	0.37	4.71	12.73	10.36	2,201	103,030	46.81	40.15	36,083	37,035	109.66
M2	1	0.35	4.92	14.06		2,314	82,098	35.48		39,572		
	2	0.39	3.76	9.64	11.84	2,276	84,717	37.22	36.35	37,056	38,314	102.52

Notes: (1) Average ultimate area (in.lbs) divided by beam weight in pounds (span length of 9 feet used to calculate total beam volume)

(2) Second instrumented SR5 beam cracked during transportation to test site

(3) Data lost due to video equipment battery failure

TABLE 7. BEAM TYPE RANKINGS. (INSTRUMENTED)

Avg. Ductility Index	Avg. Energy Ratio	Avg. Max. Load (lbs)	Energy Absorption Per Pound
M2 - 11.84	SR8 - 40.15	M2 - 38,314	SR8 - 109.66
SR6 - 11.18	SR6 - 36.40	SR8 - 37,035	M2 - 102.52
SR8 - 10.36	M2 - 36.35	SR4 - 34,238	SR4 - 92.00
SR5 - 9.39	SR4 - 31.99	SR5 - 31,669	SR6 - 86.60
SR4 - 8.46	SR5 - 31.75	SR6 - 30,594	SR5 - 79.72

TABLE 8. NORMALIZED BEAM TYPE RANKINGS (INSTRUMENTED).

Beam ID	Avg. Ductility Index	Avg. Energy Ratio	Energy Absorption Per Pound
SR4	1.00	1.00	1.00
SR5	1.11	0.99	0.87
SR6	1.32	1.13	0.94
SR8	1.22	1.25	1.19
M2	1.39	1.14	1.11

3.2.6   Best Beam Types

On the basis of the discussion presented in Subsection 3.2.5 above, two beam types show the greatest promise for enhancing the performance of hardened structures. Specifically, these beam types are:

-    Beam Type SR8: lightweight, high-strength concrete with tension rebar reinforcement, in combination with straight, short (5/8-inch) steel fiber reinforcement (Fiber Type Steel-3 in Table 2).

-    Beam Type M2: lightweight, high-strength concrete with tension rebar reinforcement, in combination with anchorloc steel fibers and mat fiber matrix in the bottom of the beam (Fiber Types Steel-2 and Mat in Table 2).

3.3 MOMENT/LOAD CAPACITY COMPARISONS

Table 9 presents the calculated ACI ultimate moment and corresponding total beam load (see Table 3) along with actual measured total beam load and moment for each beam type. In addition, Table 9 gives the percentage difference between the calculated and measured values. As seen from the table, measured loads and moments are consistently higher than those calculated using the ACI ultimate strength design methods for concrete beams in flexure. This holds true especially for the SR8 and M2 beam types, which also were the highest performing beam types as indicated by Tables 6, 7, and 8. Even the SR4 beam type, which had no fiber reinforcement, was over-designed by almost 15-percent. All this implies that designing structural members with fiber reinforcement in combination with standard rebar reinforcement will be inherently conservative. This issue will be addressed in Phase III of this technical effort, where design methods will be optimized for lightweight, fiber-reinforced concrete beams intended for use in hardened structures.

31

TABLE 9. CALCULATED & MEASURED MOMENT/LOAD COMPARISONS. (INSTRUMENTED BEAMS)

Beam Type	ACI Ultimate Moment (in-kips)	Calculated Total Beam Load (kips)	Measured Total Beam Load (kips)	Average Measured Total Beam Load (kips)	Measured Ultimate Moment (in-kips)	Average Measured Ultimate Moment (in-kips)	% Difference Between Calculated & Measured Ultimate Moment & Load
SR4	536.5	29.8	Beam 1: 34.1 Beam 2: 34.4	34.2	Beam 1: 613.8 Beam 2: 619.2	616.5	+14.9
SR5	543.9	30.2	Beam 1: 31.7	31.7	Beam 1: 570.6	570.6	+4.9
SR6	546.8	30.4	Beam 1: 30.6	30.6	Beam 1: 550.8	550.8	+0.7
SR8	543.8	30.2	Beam 1: 38.0 Beam 2: 36.1	37.0	Beam 1: 684.0 Beam 2: 649.8	666.9	+22.6
M2	548.3	30.5	Beam 1: 39.6 Beam 2: 37.1	38.3	Beam 1: 712.8 Beam 2: 667.8	690.3	+25.9

SECTION 4

TEST RESULTS – STANDARD REBAR BEAMS

4.1 OVERVIEW

One out of the three beams of each beam type used standard Number 6 (60 ksi) rebar. The actual tested strength of the rebar was 68.5 ksi. In the SR5, SR6, SR8, and M2 beams, two Number 6 rebars were used per beam in the configuration shown in Figure 7. In addition, the M2 beam was reinforced at the bottom with a slurry-infiltrated steel fiber mat, with steel fiber-reinforced concrete above the mat. For the SR4 beam, which used both tension and compression rebar reinforcement, four Number 6 rebars were used. The rebar configuration of the SR4 beam is also shown in Figure 7. A total of eight Number 3 rebar stirrups were used for each half of the SR4 beam. For each beam half, the first stirrup was placed 3 inches from the end of the beam, with the next spaced six inches from the first. The six stirrups were spaced at 7-inch intervals. The SR4 beam acted as the control during testing. It represented current hardened structure construction practice, i.e. normal weight concrete, symmetrically reinforced with stirrup shear reinforcement. All other beam types were compared against the SR4 beam type to determine whether they offered superior performance, while providing a weight saving and allowing elimination of standard rebar shear and compression reinforcement.

4.2 TEST RESULTS

4.2.1 Load-Deflection Curves and Failure Mode

The beams were tested on the load-frame shown in Figures 1 and 2 to generate load-deflection curves for each beam type. The load-deflection curves showing total load versus mid-span, top-of-beam deflection for beam 3 of each beam type are shown in Figure 25. Typical views of the non-instrumented , standard rebar beam testing process are shown in Figures 26 to 28.

As previously stated, a major observation resulting from the testing of instrumented rebar beams was that the instrumented rebars had a direct effect on the beam failure mode (see Subsection 3.2.3). The plastic sleeve used to cover the vibrating wire strain gage in an instrumented rebar prevented bonding between the concrete and rebar at the location of the sleeve. During testing, a large crack developed in the concrete at the location of the sleeve in the instrumented beams. The crack's location corresponded roughly to the middle of the tension zone
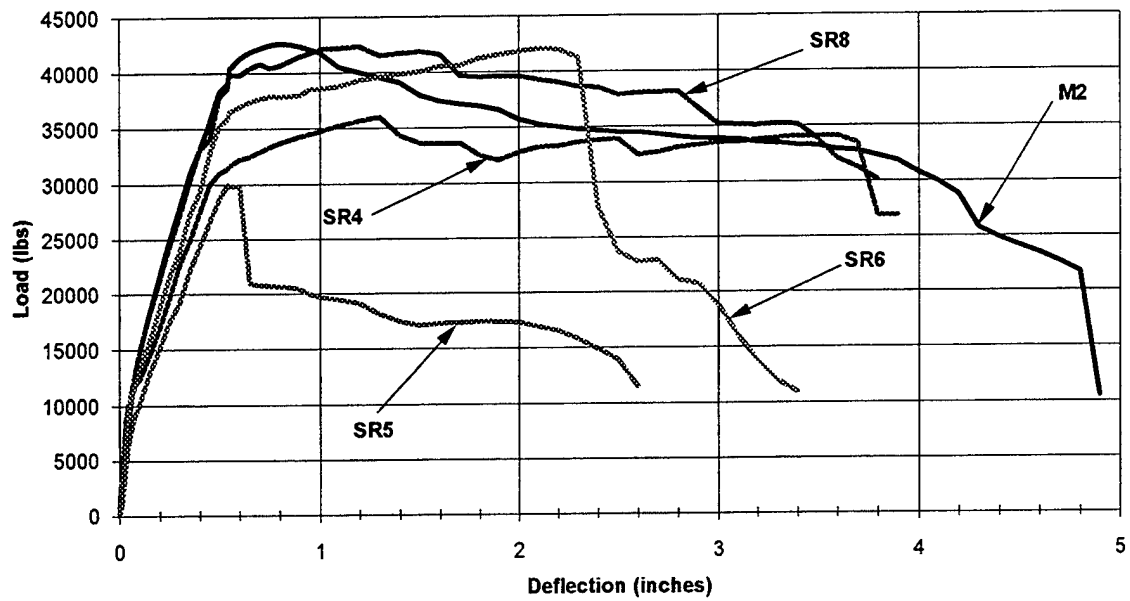
33

Figure 25. Load-Deflection Curves, Beam 3 (Non-Instrumented Rebar).
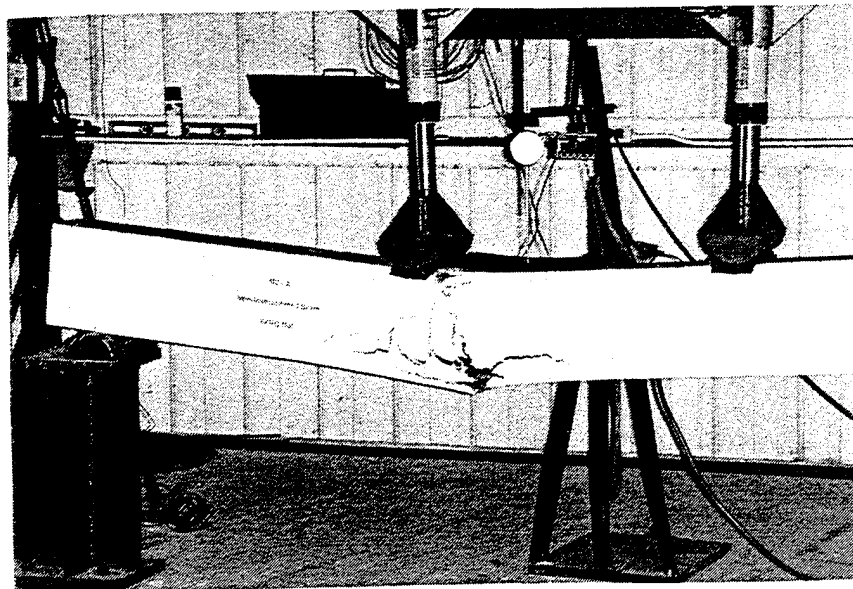

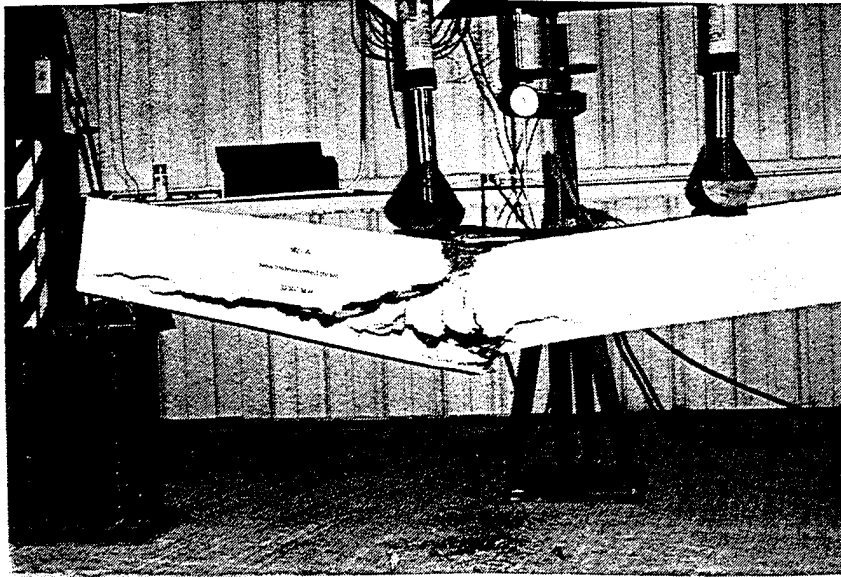Figure 26. View 1 of the Non-Instrumented Rebar Beam Testing Process.

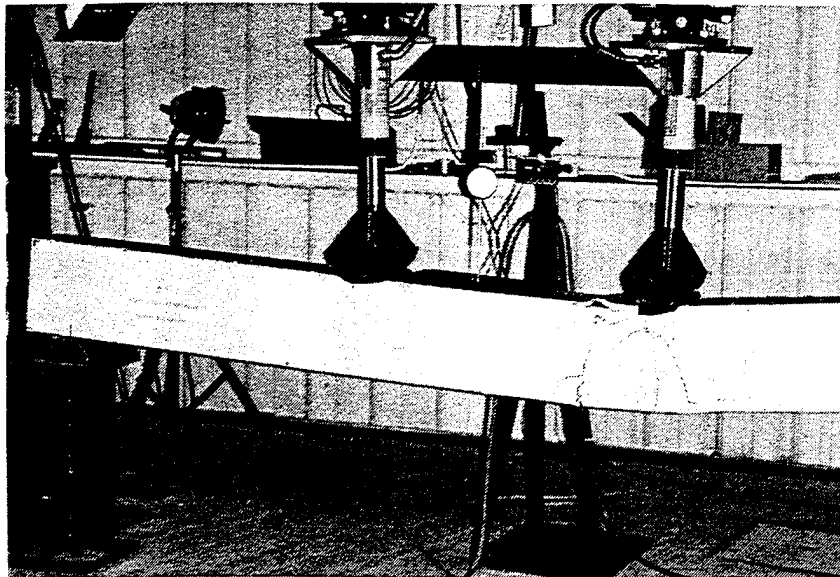Figure 27. View 2 of the Non-Instrumented Rebar Beam Testing Process.

Figure 28. View 3 of the Non-Instrumented Rebar Beam Testing Process.

between the two load points. Very little cracking was observed in the rest of an instrumented beam's tension zone.

In the beams without the instrumented rebar, distributed cracking was observed throughout the tension zone between the two load points. Because the entire tension zone between the load points was active in supporting the applied load, the capacity of the non-instrumented beams was, in general, higher than that of the instrumented beams. Two examples of the non-instrumented beam failure mode, where cracking throughout the area between the load points can be seen, are shown in Figures 29 and 30.

4.2.2 Ductility Indices And Energy Ratios

As before, the performance of the various beam types was compared using ductility indices, energy ratios, and the average total energy absorbed by a beam type measured in inch-pounds per unit beam weight. The method used to calculate ductility indices and energy ratios from load-deflection curves is shown in Figure 24 and described in Subsection 3.2.4.

4.2.3 Beam Test Results

Using the methods described in Subsection 3.2.4, ductility indices, energy ratios, and total absorbed energy per pound were calculated for each beam. As before, a span length of 9 feet was used to calculate beam weight for absorbed energy per pound calculations. Results of all these calculations are given in Table 10.

On the basis of the results shown in Table 10, each beam type was ranked by ductility index, energy ratio, maximum load, and energy absorption per pound. This information is presented in Table 11. In addition to the results presented in Table 11, ductility index, energy ratio, and energy absorption per pound results were normalized with respect to the baseline beam type SR4. This information is presented in Table 12. This information allows the beam types providing the best overall performance versus what is currently used in hardened structure construction to be readily identified. As seen from Tables 10 and 11, the same beam types that showed good results during instrumented beam testing, i.e. SR8 and M2 beam types, also showed good results during non-instrumented beam testing. Beam type M2 is the highest rated in all four categories, i.e. energy ratio, ductility index, maximum load, and energy absorption. Beam type SR8 is rated second in all four categories. The SR5 and SR6 beam types once again did not perform well. In fact, the performance of the SR5 beam was so poor it may indicate that the beam was damaged prior to testing.

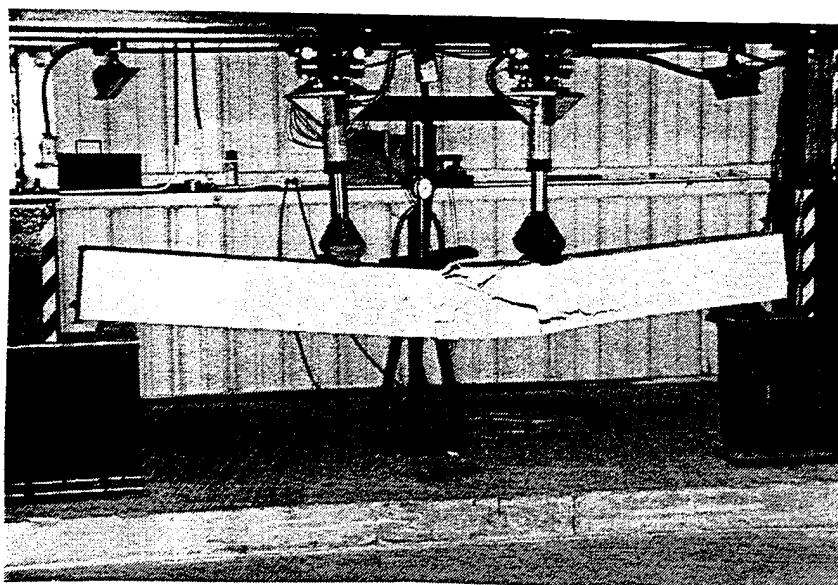Figure 29. View 1 of Non-Instrumented Rebar Beam Failure Mode.

Figure 30. View 2 of Non-Instrumented Rebar Beam Failure Mode.

TABLE 10. DUCTILITY INDICES, ENERGY RATIOS, AND ABSORBED ENERGY PER POUND FOR TEST BEAMS (NON-INSTRUMENTED).

Beam ID	Beam No.	Yield Deflc. (in)	Max. Deflc. (in)	Duct. Index	Yield Area (in.lbs)	Ult. Area (in.lbs)	Energy Ratio	Max. Load (lbs)	Energy (in.lbs) Per lb (1)
SR4	3	0.54	3.90	7.22	8,762	123,030	14.04	36,005	130.61
SR5	3	0.46	2.60	5.65	7,076	46,929	6.63	29,948	53.90
SR6	3	0.59	3.42	5.80	8,823	104,590	11.85	42,071	131.16
SR8	3	0.48	3.89	8.10	8,526	138,170	16.20	42,313	173.15
M2	3	0.44	4.97	11.30	8,323	152,180	18.28	42,636	187.05

Notes: (1) Average ultimate area (in.lbs) divided by beam weight in pounds (span length of 9 feet used to calculate total beam volume)

TABLE 11. BEAM TYPE RANKINGS (NON-INSTRUMENTED)

Ductility Index	Energy Ratio	Max. Load (lbs)	Energy Absorption Per Pound
M2 - 11.30	M2 - 18.28	M2 - 42,636	M2 - 187.05
SR8 - 8.10	SR8 - 16.20	SR8 - 42,313	SR8 - 173.15
SR4 - 7.22	SR4 - 14.04	SR6 - 42,071	SR6 - 131.16
SR6 - 5.80	SR6 - 11.85	SR4 - 36,005	SR4 - 130.61
SR5 - 5.65	SR5 - 6.63	SR5 - 29,948	SR5 - 53.90

TABLE 12. NORMALIZED BEAM TYPE RANKINGS (NON-INSTRUMENTED)

Beam ID	Ductility Index	Energy Ratio	Energy Absorption Per Pound
SR4	1.00	1.00	1.00
SR5	0.78	0.47	0.41
SR6	0.80	0.84	1.00
SR8	1.12	1.15	1.33
M2	1.57	1.30	1.43

38

Based on Table 12, which normalizes the performance of all beams against the baseline beam type SR4, the SR8 beam type's performance level was from 12- to 33-percent better than the baseline beam. The M2 beam's performance level was from 30- to 57-percent better than the baseline beam. Only the SR5 and SR6 beam types failed to exceed the SR4 beam type's performance level in any category. In fact, of the two, only the SR6 beam was able to even meet the performance level of the baseline beam, and then in only the energy absorption category.

By comparing the results from Tables 6 (instrumented beams) and Table 10 (non-instrumented beams) two conclusions can be drawn. First, the average ductility indices and energy ratios given in Table 6 are across-the-board higher than those given in Table 10. This was caused by the large crack failure mode of the instrumented beams, which increased the ductility index and energy ratio results of these beams. Remember, the ductility index equals total beam deflection divided by first crack (yield) deflection, while the energy ratio equals total load-deflection curve area divided by first crack yield area. Consequently, the earlier yielding occurs in a beam the larger are its ductility index and energy ratio, all other things being equal. This holds true especially for the energy ratio results of the instrumented beams. The yield areas given in Table 6 were much more affected by the large crack failure mode, when compared to the same results in Table 10, than were the total area under the load-deflection curve results given in the tables. Consequently, energy ratio results in Table 6 are two to five times higher than those given in Table 10.

The second conclusion is that the large crack failure mode of the instrumented beams caused their maximum loads to be lower, in all but one case, than their non-instrumented beam counterparts. Only the non-instrumented SR5 beam maximum load was lower (by 5.5-percent) than the SR5 instrumented beam type average result. In all other cases, maximum loads of the non-instrumented beams were from 5- to 37-percent higher than those of their instrumented beam counterparts. This in turn resulted in higher load-deflection curve ultimate areas for the non-instrumented beams, which caused their energy absorption results to be consistently higher than for the instrumented beams. The one exception was the SR5 beam type. As already stated, the non-instrumented SR5 beam might have been damaged prior to testing, which could be the reason why its ultimate area, maximum load, and energy absorption values in Table 10 are less than the average values given in Table 6 for the instrumented SR5 beam type.

4.2.4 Best Beam Types

Fortunately, while instrumented and non-instrumented beams failed differently and provided different performance values, the overall performance trends between the different beam types were consistent. In both cases, the clear performance leaders were the SR8 and M2 beam types. The SR5 and SR6 beam types provided only marginally better, and in some cases worse,

performance than did the baseline (control) SR4 beam type. So, based on both instrumented and non-instrumented beam testing results, the best beam types are:

- <u>Beam Type SR8</u>: lightweight, high-strength concrete with tension rebar reinforcement, in combination with straight, short (5/8-inch) steel fiber reinforcement (Fiber Type Steel-3 in Table 2).

- <u>Beam Type M2</u>: lightweight, high-strength concrete with tension rebar reinforcement, in combination with anchorloc steel fibers and mat fiber in the bottom of the beam (Fiber Types Steel-2 and Mat in Table 2).

4.3 MOMENT/LOAD CAPACITY COMPARISONS

Table 13 presents the calculated ACI ultimate moment and corresponding total beam load (see Table 3) along with actual measured total beam load and moment for each non-instrumented beam type. In addition, Table 13 gives the percentage difference between the calculated and measured values. As with the instrumented beam types, measured loads and moments for the non-instrumented beams are consistently higher, except for the SR5 beam type, than those calculated using the ACI ultimate strength design methods for concrete beams in flexure. In fact, the difference is even greater for the non-instrumented beams, because except for the SR5 beam type, their maximum loads were higher than corresponding instrumented beams. This holds true especially for the SR8 and M2 beam types. Even the SR4 beam type, which had no fiber reinforcement, was over-designed by nearly 21-percent. Once again, as with the instrumented beams, this implies that designing structural members with fiber reinforcement in combination with standard rebar reinforcement will be inherently conservative using standard ACI ultimate strength design methods. This issue will be addressed in Phase III of this technical effort, where design methods will be optimized for lightweight, fiber-reinforced concrete beams.

TABLE 13. CALCULATED & MEASURED MOMENT/LOAD COMPARISONS (NON-INSTRUMENTED BEAMS).

Beam Type	ACI Ultimate Moment (in-kips)	Calculated Total Beam Load (kips)	Measured Total Beam Load (kips)	Measured Ultimate Moment (in-kips)	% Difference Between Calculated & Measured Ultimate Moment & Load
SR4	536.5	29.8	Beam 3: 36.0	Beam 3: 648.0	+20.8
SR5	543.9	30.2	Beam 3: 29.9	Beam 3: 538.2	-1.0
SR6	546.8	30.4	Beam 3: 42.1	Beam 3: 757.8	+38.5
SR8	543.8	30.2	Beam 3: 42.3	Beam 3: 761.4	+40.1
M2	548.3	30.5	Beam 3: 42.6	Beam 3: 766.8	+39.7

SECTION 5

CONCLUSIONS AND RECOMMENDATIONS

5.1 CONCLUSIONS

Using fiber reinforcement in combination with standard reinforcement in hardened structures would provide a significant performance enhancement over the conventionally reinforced concrete structural members currently used in hardened construction. The major benefits are threefold. First, the ductility and energy absorption characteristics, i.e. material toughness, of the lightweight, fiber- and rebar-reinforced concrete SR8 and M2 beam types are clearly superior to the standard weight, symmetrically-reinforced SR4 beam type that represents current U.S. Air Force hardened structure design practice. Second, using fibers will eliminate the need for compression and shear reinforcement in lightweight concrete beams, without degrading their performance, while providing a weight saving of approximately 15-percent. Also, eliminating compression and shear reinforcement would further reduce the cost and weight of the concrete beams. Third, including fibers would minimize, or possibly eliminate, spalling of the interior walls of a hardened structure from blast loading or projectile impact.

Increasing concrete's material toughness by using fibers, while at the same time lowering the concrete's weight and cost, is especially beneficial for prefabricated, modular, rapidly erectable hardened structures designed for bare base, force projection situations. By incorporating fiber- and rebar-reinforced concrete structural members into the design of a hardened structure, the same level of protection can be obtained at a much lower weight and cost than possible using current design methods. Conversely, for the same weight and slightly lower cost a hardened structure could be designed using fiber- and rebar-reinforced structural members that are far more resistant to blast loading and impact than currently available designs.

5.2 RECOMMENDATIONS

Based on test results from Phases I (see Reference 1) and II of this research effort, using fiber reinforcement in combination with standard rebar reinforcement should be a design option for future U.S. Air Force hardened structures. This recommendation holds true especially for modular, prefabricated, rapidly erectable hardened shelters. Once Phase III of this research effort is completed, all the necessary tools and information, such as design methods and mix designs,

will be available for using fiber reinforcement in hardened structures. Finally, it is recommended that an additional phase be added to this research effort. In this Phase IV effort, scaled hardened structures should be constructed using the most promising fiber- and rebar-reinforced structural member designs identified by this technical effort. The scaled structures should be instrumented with accelerometers, pressure gauges, etc. A baseline, scaled, instrumented structure should also be constructed using current hardened construction design practices. The structures should then be subjected to blast loadings and dynamic impacts from conventional weapons, such as bombs and rockets. Based on instrumentation data, visual inspection, and deflection measurements the relative performance of the scaled structures can be determined. Successful completion of this final phase of testing should provide indisputable proof that fiber- and rebar-reinforced concrete structural members are superior to the standard rebar-only reinforced structural members currently used in U.S. Air Force hardened structures.

REFERENCES

1. Jackson, A.E. Jr., Cook, W.H., Lundstom, E., Strickland, W.S., and Knight, T., Joint Services Manual for the Design and Analysis of Hardened Structures to Conventional Weapon Effects (DAHS CWE Manual), Chapter 4, "Material Properties," U.S Army Corps of Engineers, Waterways Experiment Station, Jan. 1994.

2. Lankard, D.R., "Slurry Infiltrated Fiber Concrete (SIFCON)," Concrete International, Vol. 6, No. 12, Dec. 1984, pp 44-47.

3. Read, D.L. and Muszynski, L.C., Fiber-Reinforced Concrete for Hardened Shelter Construction, Applied Research Associates, Inc., report to the Air Force Civil Engineering Support Agency, ESL-TR-92-68, Feb 1993.

4. American Institute of Steel Construction, Manual of Steel Construction, Eighth edition, 1980.

5. American Society of Testing and Materials, ASTM C78-84, "Standard Test Method for Flexural Strength of Concrete (Using Simple Beam with Third-Point Loading)," Vol. 4.02, 1992.

6. American Society of Testing and Materials, ASTM C1018-89, "Standard Test Method for Flexural Toughness and First Crack Strength of Fiber-Reinforced Concrete(Using Simple Beam with Third-Point Loading)," Vol. 4.02, 1992.

7. Craig, R.J., "Flexural Behavior and Design of Reinforced Fiber Concrete Members," Fiber Reinforced Concrete Properties and Applications, ACI SP-105, American Concrete Institute, 1987, pp. 517-563.

8. Craig, R.J., Editor, Design with Fiber Reinforced Concrete, ACI SCM-10(85), American Concrete Institute, 1985.

9. Craig, R.J., McConnell, J., Germann, H., Dib, N., and Kashani, F., "Behavior of Reinforced Fibrous Concrete Columns," Fiber Reinforced Concrete Properties and Applications, ACI SP-105, American Concrete Institute, 1987, pp. 69-83.

10. American Concrete Institute, ACI 318-83, Building Code Requirements for Reinforced Concrete, ACI Manual of Concrete Practice, Part 3, 1987.

11. Hebda, L., Rudzinski, L., and Burakiewicz, A., "Influence of Material Structure of SFRC on Toughness Index," International Conference on Fiber Reinforced Cements and Concretes - Recent Developments, University of Wales College, U.K., 18-20 Sept., 1989, pp. 388-400. Published by Elsevier Science Publishing Co.

12. American Society of Testing and Materials, ASTM C39, "Standard Test Method for Compressive Strength of Cylindrical Specimens," Vol. 4.02, 1992.

13. Naaman, A.E., Reinhardt, H.W., and Fritz, C., "Reinforced Concrete Beams with a SIFCON Matrix," <u>American Concrete Institute Structural Journal</u>, Vol. 89, No. 1, Jan-Feb 1992, pp. 79-88.